

Entanglement renormalization of fractonic anisotropic \mathbb{Z}_N Laplacian models

Yuan Xue,^{1,*} Pranay Gorantla,^{2,†} and Zhu-Xi Luo^{3,4,‡}

¹*Department of Physics, The University of Texas at Austin, Austin, TX 78712, USA*

²*Kadanoff Center for Theoretical Physics & Enrico Fermi Institute, University of Chicago, Chicago, IL 60637, USA*

³*School of Physics, Georgia Institute of Technology, Atlanta, GA 30332, USA*

⁴*Department of Physics, Harvard University, Cambridge, MA 02138, USA*

(Dated: April 29, 2025)

Gapped fracton phases constitute a new class of quantum states of matter which connects to topological orders but does not fit easily into existing paradigms. They host unconventional features such as sub-extensive and robust ground state degeneracies as well as sensitivity to lattice geometry. We investigate the anisotropic \mathbb{Z}_N Laplacian model [1] which can describe a family of fracton phases defined on arbitrary graphs. Focusing on representative geometries where the 3D lattices are extensions of 2D square, triangular, honeycomb and Kagome lattices into the third dimension, we study their ground state degeneracies and mobility of excitations, and examine their entanglement renormalization group (ERG) flows. All models show bifurcating behaviors under ERG but have distinct ERG flows sensitive to both N and lattice geometry. In particular, we show that the anisotropic \mathbb{Z}_N Laplacian models defined on the extensions of triangular and honeycomb lattices are equivalent when N is coprime to 3. We also point out that, in contrast to previous expectations, the model defined on the extension of Kagome lattice is robust against local perturbations if and only if N is coprime to 6.

CONTENTS

I. Introduction	1	a. Gröbner basis of ideals of polynomial rings for $q = t = 1$	15
II. The polynomial framework	3	b. Alternative expression for GSD when $q = t = 1$	15
A. The polynomial formalism for stabilizer Hamiltonians	3	c. Gröbner basis of submodules of free modules for $q = t > 1$	16
B. Elementary symplectic transformations	4	d. Alternative expression for GSD when $q = t > 1$	17
C. Anisotropic extension in the polynomial formalism	5	2. \mathbb{Z}_p Laplacian model on the triangular lattice	18
III. Anisotropic \mathbb{Z}_N Laplacian model on regular lattices	5	3. \mathbb{Z}_3 fractal spin liquid	22
A. On the extended triangular lattice	6	4. \mathcal{B} code of \mathbb{Z}_3 Laplacian model on the square lattice	23
B. On the extended honeycomb lattice	7	C. Mobility of z -lineons in the triangular-based anisotropic Laplacian model	24
C. On the extended Kagome lattice	9	D. Robustness of the anisotropic Laplacian model on various regular lattices	25
IV. Entanglement renormalization of the anisotropic Laplacian models	9	References	26
A. Entanglement renormalization	10		
B. On the square lattice	11		
C. On the triangular and honeycomb lattice	12		
V. Discussion and outlook	13		
Acknowledgments	13		
A. Review of anisotropic \mathbb{Z}_N Laplacian model on the square lattice	13		
B. Ground-state degeneracies of the Laplacian models and the associated \mathcal{B} codes	14		
1. General procedure	14		

I. INTRODUCTION

Gapped fracton phases [2–5] lie at the frontier of our understanding of phases of matter [6–8]. While resembling topological phases in many aspects, they do not completely fall into the existing theoretical paradigms: for example, they also host fractionalized excitations, but with restricted mobility; they also exhibit robust ground state degeneracy (GSD) on nontrivial manifolds, but the degeneracy can be sub-extensive and is sensitive to lattice geometry. Even more intriguingly, in the cases usually referred to as type-II fractons such as Haah’s cubic code [5] (also see recent progress such as [9, 10]), there exists a sharp fluctuation of the GSD as the system size grows, which renders the definition of phases in the thermodynamic limit challenging.

* yuan_xue@utexas.edu

† gorantla@uchicago.edu

‡ zhuxi_luo@gatech.edu

One important method in modern condensed matter physics to identify phases of matter is through the entanglement renormalization (ER) [11, 12]. It is similar to the usual real-space renormalization group (RG) flow [13], but has an extra step of reducing the short-range entanglement after coarse graining. It has been successfully employed in many systems such as topological phases [12, 14], critical phenomena [15–18] and quantum fields [19]. Progresses using ER to study fracton phases will be reviewed below.

A general ER of a Hamiltonian $H(a)$ living on a lattice with lattice spacing a can be written as

$$UH(a)U^\dagger \cong H_1(ca) + H_2(ca) + \cdots + H_b(ca), \quad (1)$$

where U is a finite-depth local unitary circuit, b is the number of decoupled models and c is the coarse-graining factor. We use \cong to denote that the Hamiltonians on two sides are equivalent up to trivial Hamiltonians whose ground states are product states [20]. Conventional fixed-point topological orders or topological quantum liquids (TQL) [21], such as toric code [22], satisfy

$$UH(a)U^\dagger \cong H(ca). \quad (2)$$

In two dimensions, it is known that every translational invariant Pauli stabilizer code in 2D can be transformed to copies of 2D toric code via finite-depth local unitary transformations [23–25]. Therefore, by (2), it is equivalent to copies of 2D toric code under ER. In three dimensions, however, the existence of fracton phases in addition to topological phases leads to more possibilities than (2).

Fracton phases typically show bifurcating behaviour under ER [20, 26, 28–33], where they decouple into two independent components [34–36]. Under a particular coarse-graining, examples of exactly solvable fracton systems have been shown to be either self-bifurcating fixed points satisfying

$$UH_{SB}(a)U^\dagger \cong n \times H_{SB}(ca), \quad (3)$$

or quotient fixed points satisfying

$$UH_Q(a)U^\dagger \cong H_Q(ca) + n \times H_{SB}(ca), \quad (4)$$

where n is the number of copies. While there are many works that study the ER of foliated fracton models [26, 28–31], the ER of type-II fracton phases has been largely unexplored, with the existing studies [5, 32] focusing on \mathbb{Z}_2 qubit cases and simple lattices.

Besides the bifurcating feature, another important property distinguishing fracton orders from TQL is that the former is highly sensitive to lattice geometry. That is, the same fracton model defined on different lattices can have different low-energy properties. This is a consequence of UV/IR mixing in these models [37]. Recently, a general class of models, which can host fracton phases, have been proposed, where the Hamiltonian can be defined on a general spatial graph using the discrete Laplacian operator [1, 38–41]. The physical observables are closely related to the graph-theoretic properties:

for example, the GSD is related to the complexity of the graph and the global symmetry is identified by the Jacobian group of the graph. We will focus on one set of such Laplacian models known as the anisotropic \mathbb{Z}_N Laplacian model [1, 39]. On many regular lattices, the GSD of this model is robust against local perturbations. Moreover, it scales sub-extensively in the system size when $N = 2$, but exhibits sharp fluctuations when N is an odd prime.

In this work, we examine the anisotropic \mathbb{Z}_N Laplacian model defined on 3D lattices that are extensions of 2D regular lattices (or graphs), specifically the triangular, honeycomb, and Kagome lattices. More concretely, consider a 2D lattice on the xy plane (or a graph). Its 3D extension (extended lattice) is constructed by stacking the 2D lattices (or graphs) along the third direction, z direction. We sometimes call this the anisotropic direction. The anisotropic model is a 3D model constructed by coupling adjacent 2D models with Ising-type interactions. We analyze the GSD, mobility restrictions of excitations, and robustness for the series of models, and investigate their ERG flows. Below is a brief summary of the results.

- GSDs are computed using techniques from commutative algebra [42]. When $N = 2$, the GSD scales linearly with the system size L . When $N = p > 2$, with p prime¹, the GSD fluctuates dramatically with L . In both cases, the GSD is sensitive to the geometry of the 2D lattice.
- Mobilities of point-like excitations are analyzed using the polynomial formalism. In all these models, there always exist excitations (lineons²) that can move along the anisotropic direction. Adapting the usual terminology, we refer to a model as type-II fracton order if no excitation can move in the xy plane without creating more excitations. The models we study are type-II when $N = p > 2$.
- The \mathbb{Z}_N model on the extended triangular lattice is equivalent to that on the extended honeycomb lattice up to disentangled degrees of freedom when N is coprime to 3. Models defined on extended triangular and honeycomb lattices are robust, as expected. However, the model defined on the extended Kagome lattice is robust if and only if N is coprime to 6, again reflecting the sensitivity of the anisotropic Laplacian model to the lattice geometry.
- The ER results are summarized in Table I. All the models we study are bifurcating. When $N = 2$, consistent with the items above, the robust models on all geometries studied here bifurcate into themselves and some copies of a scale-invariant topological order. When $N = 3$, bifurcating behaviors of these robust models

¹ We always use p to denote an odd prime, while N can be an arbitrary positive integer.

² A lineon is a point-like excitation that can move only along a line.

TABLE I. Anisotropic \mathbb{Z}_N Laplacian models defined on 3D extensions of non-square 2D regular lattices and their entanglement renormalization. The original 3D anisotropic “parent” model and its “child” model after ER are abbreviated as \mathcal{A} and \mathcal{B} respectively, though we shall only show ER of their base 2D models in the main text. STC represents a stack of 2D toric code layers and FSL¹ represents the anisotropic fractal spin liquid. The model on the Kagome lattice is not robust for $N = 2, 3$, so we skip its GSD, mobility and ER. The explicit forms of these models are given in the main text.

N	2D lattice	Robust?	GSD of \mathcal{A}	Mobility on 2D lattice	ER	ER of \mathcal{B} code
2	Square	Yes	(A2)	Lineon, fracton	$\mathcal{A} + 4 \times \text{STC}$ [26]	scale-invariant
2	Triangular/Honeycomb	Yes	(32)	Lineon, fracton	$\mathcal{A} + 6 \times \text{STC}$	scale-invariant
3	Square	Yes	(A3)	Fracton	$\mathcal{A} + 2 \times \mathcal{B}$	$3 \times \mathcal{B}$
3	Triangular	Yes	(33)	Fracton	$\mathcal{A} + 12 \times \text{FSL}$	$3 \times \text{FSL}$
3	Honeycomb	Yes	(39)	Fracton	$3 \times \mathcal{A}$	N/A
2, 3	Kagome	No	-	-	-	-

¹ Here, we dub this model as “fractal spin liquid” in the sense that it is similar to the Yoshida’s fractal spin liquid model introduced in [27]. However, our model is based on qudits and defined by the stabilizer matrix in (37).

are very similar to that of the cubic code: the resultant model is the original “parent” model plus some copies of a different self-bifurcating “child” model. In particular, the anisotropic Laplacian model defined on the square or triangular lattice is a quotient fixed point while that defined on the honeycomb lattice is a self-bifurcating fixed point, again an evidence for the geometric sensitivity.

The rest of the paper is organized as follows. In Sec. II, we briefly review the polynomial formalism of \mathbb{Z}_N Pauli stabilizer Hamiltonians. In Sec. III, we review the anisotropic \mathbb{Z}_N Laplacian model on graphs and then specialize to the extended triangular, honeycomb, and Kagome lattices. The GSD, mobility of excitations, and robustness are discussed. In Sec. IV, we first review the general procedure of ER and then investigate the ER transformations of $\mathbb{Z}_{2,3}$ Laplacian models on the above extended lattices. In Appendix A, we review the properties of the anisotropic \mathbb{Z}_N Laplacian model on the square lattice. In Appendices B, C, and D, we analyze the GSDs, mobilities of excitations, and robustness, respectively, of the models discussed in the main text.

II. THE POLYNOMIAL FRAMEWORK

A. The polynomial formalism for stabilizer Hamiltonians

Any translation-invariant stabilizer Hamiltonian can be expressed conveniently in the polynomial formalism [27, 42], which we will use heavily in this work. In this section, we review the basic ideas of this algebraic representation of stabilizer Hamiltonians.

A stabilizer Hamiltonian that includes q types of \mathbb{Z}_N qudits at each site and t types of stabilizers can be written as a $2q \times t$ matrix, denoted as \mathcal{A} or \mathcal{B} in this paper, whose entries are polynomials with coefficients in \mathbb{Z}_N , i.e., integers modulo N . Each column corresponds to one of the t stabilizers. More

concretely, working in two spatial dimensions, we have the map

$$\begin{pmatrix} f_1(x, y) \\ \vdots \\ f_q(x, y) \\ g_1(x, y) \\ \vdots \\ g_q(x, y) \end{pmatrix} \mapsto \prod_{i=1}^q S_{Z,i}(f_i) S_{X,i}(g_i), \quad (5)$$

where f_i ’s and g_i ’s are polynomials, and

$$\begin{aligned} S_{Z,i}(\sum_{n,m} c_{n,m} x^n y^m) &= \prod_{n,m} Z_{i,(n,m)}^{c_{n,m}}, \\ S_{X,i}(\sum_{n,m} c_{n,m} x^n y^m) &= \prod_{n,m} X_{i,(n,m)}^{c_{n,m}}. \end{aligned} \quad (6)$$

Here, $Z_{i,(n,m)}$ and $X_{i,(n,m)}$ are the \mathbb{Z}_N Pauli clock and shift matrices, respectively, acting on the i -th qudit at site (n, m) . They satisfy the algebra $Z^N = X^N = 1$ and $ZX = e^{2\pi i/N} XZ$. Note that each monomial $x^n y^m$ corresponds to the position (n, m) of a qudit and its coefficient $c_{n,m}$ corresponds to the exponent of Z or X in the associated stabilizer term. Also, the i -th row of the first q rows and the i -th row of the last q rows represent the parts of the stabilizers that act on the i -th qudit. We use R_i^Z to denote the first q rows of the stabilizer matrix, R_i^X to denote the last q rows, and C_μ to denote the columns. The horizontal line separates the Z -type and X -type operators in each stabilizer.

Let λ be the $2q \times 2q$ matrix given by

$$\lambda = \left(\begin{array}{c|c} 0 & \mathbf{1}_q \\ \hline -\mathbf{1}_q & 0 \end{array} \right), \quad (7)$$

where $\mathbf{1}_q$ is the $q \times q$ identity matrix and the 0's are zero matrices of appropriate dimension. The fact that all the local terms in a stabilizer Hamiltonian commute with each other is codified into the equation

$$\mathcal{A}^\dagger \lambda \mathcal{A} = 0, \quad (8)$$

where $\mathcal{A}^\dagger = \overline{\mathcal{A}}^\top$ and $\overline{\mathcal{A}}$ is the matrix obtained from \mathcal{A} by replacing $x \rightarrow \bar{x} = x^{-1}$, $y \rightarrow \bar{y} = y^{-1}$, and so on.

In the following, we restrict to those Hamiltonians whose stabilizers are all either Z -type or X -type, i.e., each stabilizer involves either only Z operators or only X operators. They are known as CSS codes [43, 44]. In the polynomial formalism, the stabilizer matrix of such models is of the form

$$\mathcal{A} = \begin{pmatrix} \mathcal{A}^Z & 0 \\ 0 & \mathcal{A}^X \end{pmatrix}. \quad (9)$$

As an example, consider the 2D \mathbb{Z}_2 toric code [22] on the square lattice. Its stabilizers are given by

$$\begin{array}{cc} IZ - II & IX - XX \\ | & | \\ ZZ - ZI & II - XI \end{array}, \quad (10)$$

where ZZ is shorthand for $Z_1 Z_2$ with Z_1 acting on the first qubit at the site and Z_2 acting on the second qubit at the same site; similarly XI stands for $X_1 I_2$. In the polynomial formalism, the monomials associated with the four vertices of a plaquette can be taken as

$$\begin{array}{c} y - xy \\ | \\ 1 - x \end{array}. \quad (11)$$

Therefore, the stabilizer matrix of the toric code is given by

$$\mathcal{A}_{\text{TC}} = \begin{pmatrix} 1+x & 0 \\ 1+y & 0 \\ 0 & x+xy \\ 0 & y+xy \end{pmatrix}. \quad (12)$$

where the first (second) column corresponds to the Z -type (X -type) stabilizer in (10).

Using the fact that $x\bar{x} = 1$, $y\bar{y} = 1$, and by translation invariance, we can transform the above matrix into the equiv-

alent form

$$\begin{pmatrix} 1+x & 0 \\ 1+y & 0 \\ 0 & 1+\bar{y} \\ 0 & 1+\bar{x} \end{pmatrix}, \quad (13)$$

by multiplying the second column by $\bar{x}\bar{y}$. This operation corresponds to shifting the X -stabilizer one step along both $-x$ and $-y$ directions.

B. Elementary symplectic transformations

In [42], it was proved that two equivalent Pauli stabilizer models can be connected by a local unitary, known as a symplectic transformation³. Each symplectic transformation is a composition of some elementary row or column operations [23] that are listed below. Note that while all of them preserve the stabilizer group, and hence the ground states, some of them change the Hamiltonian, and hence the excitations.

There are three kinds of row operations⁴.

1. First, we have

$$\text{CNOT}(i, j, f) : \begin{array}{l} R_i^X \mapsto R_i^X + f R_j^X, \\ R_j^Z \mapsto R_j^Z - \bar{f} R_i^Z, \end{array} \quad (14)$$

where f is a polynomial. As indicated, this is implemented by controlled-NOT (CNOT) gates where the target qudits are specified by i and f , and the control qudit is the j -th qudit.

2. Next, we have

$$R_i^X \mapsto x^n y^m R_i^X, \quad R_i^Z \mapsto x^n y^m R_i^Z. \quad (15)$$

This corresponds to translating the i -th qudit by (n, m) in each stabilizer.

3. And finally, we have

$$R_i^X \mapsto k R_i^X, \quad R_i^Z \mapsto r R_i^Z, \quad (16)$$

where k, r are integers such that $kr = 1 \pmod{N}$. This corresponds to replacing $X_i \rightarrow X_i^k$ and $Z_i \rightarrow Z_i^r$ in each stabilizer. The choice of k and r ensures that the new set of stabilizers still commute with each other. Note that this operation is trivial for qubits.

³ The name is inspired by the fact that the corresponding polynomial matrix is a symplectic matrix that preserves λ .

⁴ Ref. [23] mentions other elementary row operations based on the controlled-phase (CPhase) gate and the Hadamard gate, but we do not use them because they spoil the structure (9) of the stabilizer matrix.

Similarly, there are three kinds of column operations. First, we can multiply a column C_ν by a polynomial f and add it to another column C_μ , i.e.

$$\text{Col}(\mu, \nu, f) : C_\mu \mapsto C_\mu + f C_\nu. \quad (17)$$

Clearly, this amounts to redefining the stabilizer generators. Next, we can translate a stabilizer by (n, m) by multiplying the associated column by $x^n y^m$. And finally, we can multiply a column by an integer that has an inverse modulo N . The third operation is trivial for qubits.

C. Anisotropic extension in the polynomial formalism

Consider a stabilizer Hamiltonian described by the $2q \times t$ matrix

$$\mathcal{A} = \begin{pmatrix} \mathcal{A}_{q \times t}^Z \\ 0 \end{pmatrix}, \quad (18)$$

where the 0 in the bottom row is understood to be a zero matrix of size $q \times t$. The form of this matrix implies that all stabilizers are of Z -type. Moreover, it satisfies (8) trivially. An example of this type is the 1D Ising model without the transverse-field term, which has the stabilizer matrix

$$\mathcal{A}_{\text{Is}} = \begin{pmatrix} 1+x \\ 0 \end{pmatrix}. \quad (19)$$

Such models are commonly referred to as “classical codes” (see, for example, [27]).

When $q = t$, one can define the anisotropic extension of the classical code as the stabilizer code given by the $4t \times 2t$ matrix

$$\mathcal{A}_{\text{ext}} = \begin{pmatrix} \mathcal{A}_{t \times t}^Z & 0 \\ (1-z)\mathbf{1}_t & 0 \\ 0 & (1-\bar{z})\mathbf{1}_t \\ 0 & -(\mathcal{A}^Z)_{t \times t}^\dagger \end{pmatrix}. \quad (20)$$

Here, z is the coordinate along the extended/anisotropic direction and the polynomial $1 - z$ corresponds to Ising-type interactions between adjacent classical codes. It is easy to verify that \mathcal{A}_{ext} satisfies (8)

For example, the 2D toric code is an anisotropic extension of the 1D Ising model along the y direction. This is easily seen by comparing (13) with the anisotropic extension of (19) and interpreting y as the anisotropic direction.

The GSDs of a classical code \mathcal{A} and its anisotropic extension \mathcal{A}_{ext} are related as

$$\text{GSD}_{\mathcal{A}_{\text{ext}}} = \text{GSD}_{\mathcal{A}}^2. \quad (21)$$

This follows from a doubling of the number of logical oper-

ators from the classical code to its anisotropic extension. For example, the 1D Ising model on a periodic chain is two-fold degenerate while the GSD of the 2D toric code on a periodic square lattice is 4, which is indeed 2^2 .

As the structure of the stabilizer matrix (20) suggests, the anisotropic extension of a classical code enjoys a self-duality that exchanges the Z -type and X -type stabilizer terms. In the example of the 2D toric code, this is the well-known e - m duality that exchanges the e and m anyons.

III. ANISOTROPIC \mathbb{Z}_N LAPLACIAN MODEL ON REGULAR LATTICES

The anisotropic \mathbb{Z}_N Laplacian model [1, 39] is a stabilizer code defined on the lattice $\Gamma \times C_{L_z}$ where Γ is a simple, connected, undirected graph, and C_{L_z} is a cycle graph (a circle along the z -direction) with the number of lattice sites in the z -direction being L_z . We use (i, z) to label the sites of the lattice and $(i, z + \frac{1}{2})$ to label the z -links. We also use $\langle i, j \rangle$ to denote an edge of the graph Γ .

There are two sets of qudits: one on the sites of the lattice, the other on the z -links connecting graphs with adjacent z -coordinates. The Hamiltonian is given by

$$H = -\gamma_1 \sum_{i,z} G(i, z) - \gamma_2 \sum_{i,z} F(i, z + \frac{1}{2}) + \text{h.c.}, \quad (22)$$

where

$$\begin{aligned} G(i, z) &= X_{z, (i, z + \frac{1}{2})}^\dagger X_{z, (i, z - \frac{1}{2})} \prod_{j: \langle i, j \rangle \in \Gamma} X_{(i, z)} X_{(j, z)}^\dagger, \\ F(i, z + \frac{1}{2}) &= Z_{(i, z+1)}^\dagger Z_{(i, z)} \prod_{j: \langle i, j \rangle \in \Gamma} Z_{z, (i, z + \frac{1}{2})} Z_{z, (j, z + \frac{1}{2})}^\dagger. \end{aligned} \quad (23)$$

Here $Z_{(i, z)}$, $X_{(i, z)}$ are the \mathbb{Z}_N clock and shift operators acting on the qudit on the site (i, z) , whereas $Z_{z, (i, z + \frac{1}{2})}$, $X_{z, (i, z + \frac{1}{2})}$ act on the qudit on the z -link $(i, z + \frac{1}{2})$.

The ground states of the anisotropic Laplacian model satisfy $G = F = 1$. To count the number of ground states, we need to count the number of independent logical operators. The logical operators take the following form⁵:

$$\begin{aligned} W_z(i) &= \prod_z Z_{z, (i, z + \frac{1}{2})}, \quad \tilde{W}_z(i) = \prod_z X_{(i, z)}, \\ W(h; z) &= \prod_i Z_{(i, z)}^{h(i)}, \quad \tilde{W}(h; z + \frac{1}{2}) = \prod_i X_{z, (i, z + \frac{1}{2})}^{h(i)}, \end{aligned} \quad (24)$$

where $h(i)$ is a \mathbb{Z}_N -valued discrete harmonic function on the graph, i.e.,

$$\Delta_L h(i) = \sum_{j: \langle i, j \rangle \in \Gamma} [h(i) - h(j)] = 0 \pmod{N}. \quad (25)$$

⁵ It is straightforward to check that they commute with the stabilizers of anisotropic Laplacian models

Here, Δ_L is the discrete Laplacian operator. By counting the number of independent Heisenberg algebras formed by these logical operators, it was shown in [1] that the GSD depends only on the graph Γ and is given by

$$\text{GSD} = \prod_{a=1}^N \gcd(N, r_a)^2 = |\text{Jac}(\Gamma, N)|^2, \quad (26)$$

where r_a 's are the invariant factors in the Smith normal form of the Laplacian matrix of Γ , $|\text{Jac}(\Gamma, N)|$ is the order of the mod- N reduction of the Jacobian group of Γ , and N is the number of vertices of Γ . The square comes from the fact that we have two sets of Heisenberg algebras $\{W_z, \tilde{W}(h)\}$ and $\{W(h), \tilde{W}_z\}$.

Note that the anisotropic Laplacian model is the anisotropic extension of the Laplacian model along the z direction. The Laplacian model is a classical code defined on the graph Γ by the Hamiltonian

$$H = -\gamma \sum_i \prod_{j: \langle i, j \rangle \in \Gamma} Z_i Z_j^\dagger + \text{h.c.}, \quad (27)$$

where Z_i is the \mathbb{Z}_N clock operator acting on the qudit on the vertex i of the graph Γ .

The anisotropic Laplacian model has point-like excitations, which are violations of the stabilizers G and F . Due to the self-duality that exchanges the G and F terms, these two kinds

of excitations have the same mobility. In particular, they are both z -lineons because they can move in the z -direction via open versions of the string operators W_z and \tilde{W}_z , respectively. However, their mobility along the graph is nontrivial and is closely related to the mobility of the point-like excitations in the Laplacian model.

A. On the extended triangular lattice

In this section, we consider the anisotropic \mathbb{Z}_N Laplacian model on the extended triangular lattice, referred to as the triangular-based anisotropic Laplacian model. Geometry of the 3D lattice is shown in Fig. 1. Periodic boundary conditions are implemented such that $(x, y, z) \sim (x + L_x, y, z) \sim (x, y + L_y, z) \sim (x, y, z + L_z)$. And the stabilizer terms (23) are given by

$$\begin{aligned} G_{\text{tri}}(\mathbf{i}, z) &= X_{z, (\mathbf{i}, z + \frac{1}{2})}^\dagger X_{z, (\mathbf{i}, z - \frac{1}{2})} X_{(\mathbf{i}, z)}^6 \prod_{j \in \mathcal{O}} X_{(j, z)}^\dagger, \\ F_{\text{tri}}(\mathbf{i}, z + \frac{1}{2}) &= Z_{(\mathbf{i}, z + 1)}^\dagger Z_{(\mathbf{i}, z)} Z_{z, (\mathbf{i}, z + \frac{1}{2})}^6 \prod_{j \in \mathcal{O}} Z_{z, (j, z + \frac{1}{2})}^\dagger, \end{aligned} \quad (28)$$

where the product is taken over the six nearest-neighbouring sites around the site \mathbf{i} . The stabilizers can be rewritten in terms of polynomial matrix⁶,

$$\mathcal{A}_{\text{tri}} = \begin{pmatrix} 6 - (x + y + \bar{x} + \bar{y} + x\bar{y} + \bar{x}\bar{y}) & 0 \\ 1 - z & 0 \\ 0 & 1 - \bar{z} \\ 0 & -6 + (x + y + \bar{x} + \bar{y} + x\bar{y} + \bar{x}\bar{y}) \end{pmatrix}. \quad (29)$$

When $N = 2$, in addition to the string-like logical operators W_z and \tilde{W}_z in the z direction, there are string-like logical operators in the xy plane:

$$\tilde{W}_C(z + \frac{1}{2}) = \prod_{(n, m) \in C} X_{z, (n, m, z + \frac{1}{2})}, \quad (30)$$

where C is a (non-contractible) rigid straight line through the sites in the $(0, 1)$, $(1, 0)$, or $(1, -1)$ direction. The number of such lines is L_x , L_y , and $\gcd(L_x, L_y)$, respectively. Similarly, there are string-like logical operators W_C for each such curve. Moreover, the logical operators \tilde{W}_C are independent of each

other except for the two relations

$$\prod_{C_y} \tilde{W}_{C_y} = \prod_{C_x} \tilde{W}_{C_x} = \prod_{C_{x\bar{y}}} \tilde{W}_{C_{x\bar{y}}} = \prod_{n, m} X_{z, (n, m, z + \frac{1}{2})}, \quad (31)$$

where C_y , C_x , and $C_{x\bar{y}}$ are the straight lines in the $(0, 1)$, $(1, 0)$, and $(1, -1)$ directions, respectively. Together with the W_z and \tilde{W}_z operators, they lead to a GSD given by

$$\log_2 \text{GSD}_{\text{tri}} = 2[L_x + L_y + \gcd(L_x, L_y) - 2]. \quad (32)$$

When $N > 2$, there is no simple structure to the logical operators in the xy plane. Instead, we calculate the ground-state degeneracy using the techniques from commutative algebra.

In particular, we show that when $N = p$ is an odd prime, for $L_x = p^{k_x} q^m$ and $L_y = p^{k_y} q^m$, where $k_x, k_y, m \geq 0$ are integers and $q \neq p$ is another odd prime such that p is a

⁶ From (22), we notice that there are four terms meaning that the stabilizer matrix should be 4×4 . However we can apply the column operations introduced in Sec. II B to eliminate one of F and F^\dagger , as well as one of G and G^\dagger . So the matrix is reduced to 4×2 . In the following, we will always use this elimination.

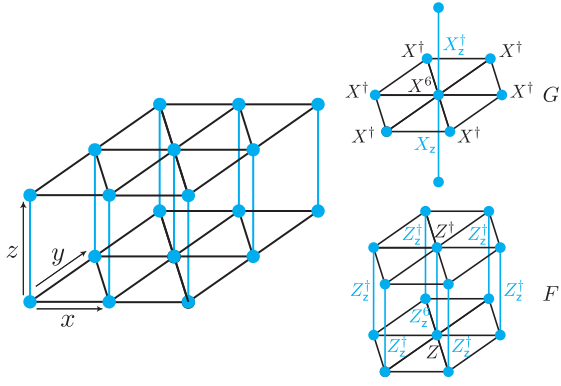


FIG. 1. The prismatic lattice $\Gamma \times C_{L_z}$, when the base graph Γ is the 2D triangular lattice, with periodic boundary conditions. C_{L_z} is shown as the blue links along z direction. The two stabilizer generators are shown as G and F . The blue variables are on the blue links (z -links) while the black ones are on the blue vertices (sites).

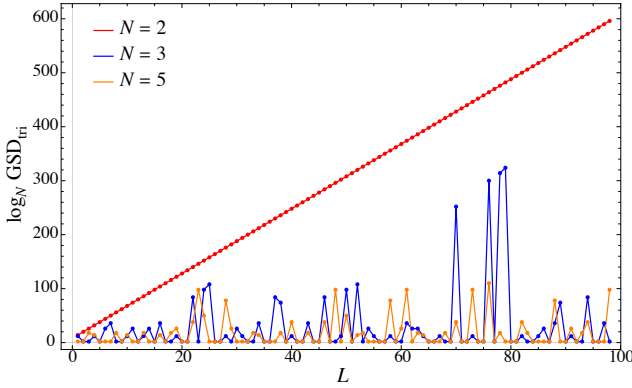


FIG. 2. The logarithm of the ground-state degeneracy of the triangular-based anisotropic \mathbb{Z}_N Laplacian model for $N = 2$ (red), 3 (blue) and 5 (orange). The system size is taken to be $L \times L \times L_z$ with $3 \leq L \leq 100$. When $N = 2$, \log_2 GSD grows linearly in L . However, when $N = 3, 5$, we see that \log_N GSD fluctuates sharply with L .

primitive root modulo q^m for $m \geq 1$, we have

$$\log_p \text{GSD}_{\text{tri}} = \begin{cases} 4 \times 3^{\min(k_x, k_y)}, & p = 3, \\ 2[2p^{\min(k_x, k_y)} - \delta_{k_x, k_y}], & p > 3. \end{cases} \quad (33)$$

See Appendix B for details⁷. The numerical calculation of GSD is shown in Fig. 2. The dramatic fluctuation of GSD with the system size when $p > 2$ suggests type-II fracton order, which we confirm by studying the mobility of excitations below.

As explained before, the triangular-based anisotropic Laplacian model has string-like logical operators along the

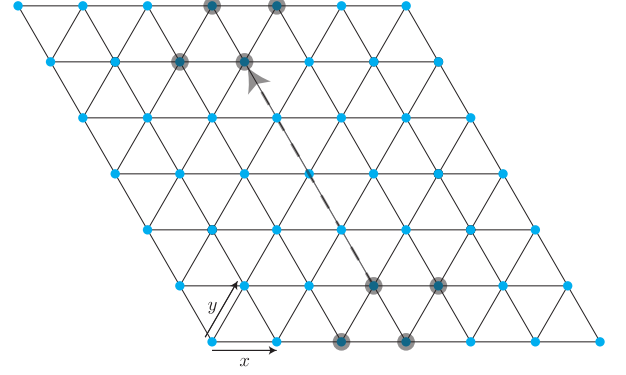


FIG. 3. The mobility of quadrupole of z -lineons (gray dots) in the triangular-based anisotropic \mathbb{Z}_2 Laplacian model. The gray dashed arrow in the $(-1, 1)$ direction indicates the string operator that moves the quadrupole located at relative positions $(0, 0)$, $(1, 0)$, $(0, 1)$, and $(1, 1)$. This string operator is an open version of the logical operator W_C or \tilde{W}_C .

z -directions, and therefore hosts z -lineons. The mobility of z -lineons on the 2D base lattice depends on N . For $N = 2$, while a single z -lineon is immobile, a quadrupole of z -lineons can move along a line as depicted in Fig. 3. This is related to the existence of the string-like logical operators W_C and \tilde{W}_C in the xy plane, whose open versions “move” a quadrupole of z -lineons that violate G and F terms, respectively. On the other hand, for $N = p$ an odd prime, any finite set of z -lineons cannot move, unless they are created locally. We prove these statements in Appendix C.

Lastly, we examine the robustness of the triangular-based anisotropic Laplacian model following the discussion in [1]. A model is robust if there are no local deformations of the Hamiltonian that commute with the Hamiltonian and lift the ground state degeneracy, i.e., if there are no logical operators with local (finite) support in the thermodynamic (infinite volume) limit.

Recall that the logical operators take the form (24). Obviously, $W_z(i)$ and $\tilde{W}_z(i)$ are supported over L_z so they have infinite support in this limit. To investigate the behaviour of $W(h)$ and $\tilde{W}(h)$ at a fixed z , we turn to look at the discrete harmonic function $h(i) = h(x, y)$ because the support of these logical operators is the same as the support of $h(x, y)$. On the infinite triangular lattice, there is no nontrivial finitely supported discrete harmonic function. We prove this fact in Appendix D. Therefore, $W(h)$ and $\tilde{W}(h)$ do not have local support, and hence the triangular-based anisotropic Laplacian model is robust.

B. On the extended honeycomb lattice

Now we turn to discuss the anisotropic Laplacian model based on the honeycomb lattice. Again, we take the prismatic lattice with periodic boundary conditions shown in Fig. 4. Notice that there are two sublattices A and B so we have two different types of stabilizers $F_{A,B}$ and $G_{A,B}$. We denote the

⁷ Throughout Appendix B, we calculate the GSD of the (classical) Laplacian model. The GSD of the anisotropic Laplacian model follows from the relation (21).

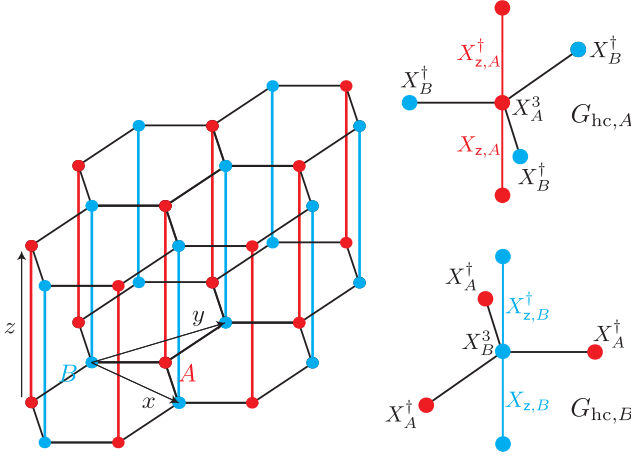


FIG. 4. The prismatic lattice $\Gamma \times C_{L_z}$ whose base graph Γ is the 2D honeycomb lattice with periodic boundary conditions. The two sublattices A and B are shown as the red and blue dots, and the z -links are colored accordingly. For each sublattice i , there are two conjugate stabilizers: $G_{hc,i}$ and $F_{hc,i}$ (we show only the former). As before, the colored variables are on the z -links, whereas the black variables are on the sites.

\mathbb{Z}_N variables living on the sublattice A as $X_{z,A}$ ($Z_{z,A}$) and X_A (Z_A) and similarly for the other sublattice. Then the stabilizers on the A sublattice are given as

$$G_{hc,A}(i, z) = X_{z,A}^\dagger(i, z + \frac{1}{2}) X_{z,A}(i, z - \frac{1}{2}) X_{z,A}^3(i, z) \prod_{j \in \Delta} X_B^\dagger(j, z),$$

$$F_{hc,A}(i, z + \frac{1}{2}) = Z_{z,A}^\dagger(i, z + 1) Z_{z,A}(i, z) Z_{z,A}^3(i, z + \frac{1}{2})$$

$$\times \prod_{j \in \Delta} Z_{z,B}^\dagger(j, z + \frac{1}{2}),$$
(34)

where the product is taken over the three nearest-neighbouring sites j around the site i , and similarly for $G_{hc,B}$ and $F_{hc,B}$. In the polynomial formalism, the Hamiltonian is associated with the matrix

$$\mathcal{A}_{hc} = \begin{pmatrix} 3 & -1 - \bar{x} - \bar{y} & 0 & 0 \\ -1 - x - y & 3 & 0 & 0 \\ 1 - z & 0 & 0 & 0 \\ 0 & 1 - z & 0 & 0 \\ \hline 0 & 0 & 1 - \bar{z} & 0 \\ 0 & 0 & 0 & 1 - \bar{z} \\ 0 & 0 & -3 & 1 + \bar{x} + \bar{y} \\ 0 & 0 & 1 + x + y & -3 \end{pmatrix}.$$
(35)

When N is coprime to 3, the honeycomb anisotropic \mathbb{Z}_N Laplacian model is equivalent to that on the triangular lattice, and hence should share the same properties. The explicit sequential local unitary transformation that relates these two

models is given by

$$\begin{aligned} & \text{Col}(2, 1, k(1 + \bar{x} + \bar{y})) \text{Col}(4, 3, k(1 + \bar{x} + \bar{y})) \\ & \times \text{CNOT}(3, 4, -k(1 + \bar{x} + \bar{y})) \\ & \times \text{CNOT}(3, 1, -k(1 - z)) \\ & \times \text{CNOT}(2, 1, k(1 + x + y)), \end{aligned}$$
(36)

where k is an integer given by $3k = 1 \pmod N$. We further multiply the first and seventh rows by k , and second and eighth rows by 3, which is complemented by multiplying the fifth and third rows by 3, and sixth and fourth rows by k . Ignoring two decoupled sets of qudits leaves two blocks which, after a rearrangement, form the stabilizer matrix of the anisotropic triangular-based Laplacian model (29).

For $N = 3$, the monomial entry 3 is reduced to 0, and the honeycomb-based anisotropic Laplacian model is decoupled into two copies of the 3+1D anisotropic \mathbb{Z}_3 fractal spin liquid (FSL) with the stabilizer matrix

$$\mathcal{A}_{\text{FSL}} = \begin{pmatrix} 1 + x + y & 0 \\ 1 - z & 0 \\ \hline 0 & 1 - \bar{z} \\ 0 & -1 - \bar{x} - \bar{y} \end{pmatrix},$$
(37)

which is the anisotropic extension of the 2D fractal spin liquid model with stabilizer matrix $(1 + x + y, 0)^\top$.

In Appendix B, we calculate the GSD of the anisotropic \mathbb{Z}_3 fractal spin liquid as

$$\log_3 \text{GSD}_{\text{FSL}} = 2 \times 3^{\min(k_x, k_y)},$$
(38)

where k_x and k_y are defined the same as in (33). The GSD of \mathbb{Z}_3 honeycomb anisotropic Laplacian is thus given by

$$\log_3 \text{GSD}_{hc} = 4 \times 3^{\min(k_x, k_y)}.$$
(39)

Curiously, this GSD matches with the GSD of the triangular-based anisotropic \mathbb{Z}_3 Laplacian model for these special values of L_x and L_y . However, numerical computation shows that they do not always match for other values of L_x and L_y . Therefore, the two models are not equivalent for $N = 3$. The numerical plot of the GSD_{hc} is shown in Fig. 5.

The mobility of z -lineons in this model is similar to that of the triangular-based anisotropic Laplacian model when N is coprime to 3. For example, when $N = 2$, a dipole of z -lineons can move in the direction orthogonal to its orientation in the xy plane as depicted in Fig. 6. Relatedly, similar to (30), there are string-like logical operators in the xy plane:

$$\tilde{W}_C(z + \frac{1}{2}) = \prod_{\ell \in C} X_{z,A}(\ell, z + \frac{1}{2}) X_{z,B}(\ell, z + \frac{1}{2}),$$
(40)

where C is a rigid straight line through the centers of the hexagons in the $(0, 1)$, $(1, 0)$, or $(1, -1)$ direction, the product is over all links ℓ pierced by C , and $X_{z,A}(\ell, z + \frac{1}{2})$ and $X_{z,B}(\ell, z + \frac{1}{2})$ act on the two qubits at the ends of the link

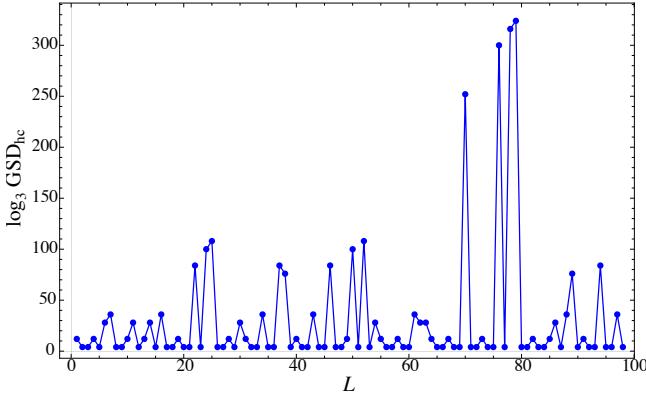


FIG. 5. The logarithm of the ground-state degeneracy of the honeycomb-based anisotropic \mathbb{Z}_3 Laplacian model on the $L \times L \times L_z$ lattice with $3 \leq L \leq 100$. It is clear that there is a dramatic fluctuation of GSD with increasing L .

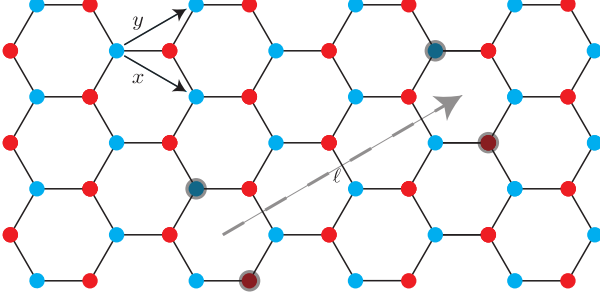


FIG. 6. The mobility of a dipole of z -lineons (gray dots) in the honeycomb-based anisotropic \mathbb{Z}_2 Laplacian model. The dashed line represents the open version of the string-like logical operator W_C or \tilde{W}_C .

ℓ . Similarly, there are string-like logical operators W_C . The open versions of W_C and \tilde{W}_C “move” the dipoles of z -lineons that violate G and F terms, respectively, as in Fig. 6.

For $N = 3$, by the same argument as in Appendix C, it is straightforward to show that any finite set of z -lineons is immobile in the xy plane, except when they are created locally. This result follows from the fact that $x^{n_0}y^{m_0} - 1$ is not a multiple of $f(x, y) = 1 + x + y \pmod{3}$.

The robustness of the anisotropic Laplacian model on honeycomb lattice follows from the same argument as that on the triangular lattice, which is spelled out in Appendix D.

C. On the extended Kagome lattice

We now turn to the anisotropic Laplacian model based on the Kagome lattice, which contains three sublattices A , B and C as shown in Fig. 7. Using the similar conventions in Sec. III B, we denote \mathbb{Z}_N operators as $X_{z,i}$ ($Z_{z,i}$) and X_i (Z_i) where $i = A, B, C$. The stabilizers on the sublattice A can be

written as

$$\begin{aligned} G_{K,A}(i, z) &= X_{z,A,(i,z+\frac{1}{2})}^\dagger X_{z,A,(i,z-\frac{1}{2})} X_{A,(i,z)}^4 \\ &\times \prod_{j \in \square} X_{B/C,(j,z)}^\dagger, \\ F_{K,A}(i, z + \frac{1}{2}) &= Z_{A,(i,z+1)}^\dagger Z_{A,(i,z)} Z_{z,A,(i,z+\frac{1}{2})}^4 \\ &\times \prod_{j \in \square} Z_{z,B/C,(j,z+\frac{1}{2})}^\dagger, \end{aligned} \quad (41)$$

where the product is taken over the four nearest-neighbouring sites around the site i and similarly for the stabilizers defined on the other two sublattices.

Contrary to what was discussed in the Footnote 15 of [1], the anisotropic Laplacian model based on the Kagome lattice is not robust for all N . A powerful test of robustness is the growth of the ground-state degeneracy with system size. It is shown in [45] that the logarithm of the ground-state degeneracy for systems with homogeneous topological order on an arbitrary closed Riemannian manifold of spatial dimension D cannot grow faster than L^{D-2} , where L is the linear size of the system. When $D = 3$, \log_N GSD is restricted from growing faster than linearly in L . We find that the Kagome anisotropic $\mathbb{Z}_{2,3}$ Laplacian model violates this bound (see the red and blue plots in Fig. 8). Upon examining the logical operators more closely, we find that there exist local operators that commute with all terms of the Hamiltonian in the $\mathbb{Z}_{2,3}$ model. They are shown as G'_K in the lower-right panel in Fig. 7(b). Similarly, there are operators F'_K that also commute with all terms of the Hamiltonian. More generally, $(G'_K)^k$ and $(F'_K)^k$ are local logical operators whenever $N = 2k$ or $N = 3k$, i.e., whenever N is a multiple of 2 or 3.

On the other hand, looking at $N = 5$ in the inset of Fig. 8, we see that \log_N GSD is bounded by a linear function of L , suggesting that the \mathbb{Z}_5 model is robust. Indeed, we prove in Appendix D that the \mathbb{Z}_N model has no local logical operators when N is coprime to 6.

It follows from the last two paragraphs that the Kagome-based anisotropic \mathbb{Z}_N Laplacian model is robust if and only if N is coprime to 6.

IV. ENTANGLEMENT RENORMALIZATION OF THE ANISOTROPIC LAPLACIAN MODELS

In this section, we study the entanglement renormalization of the anisotropic \mathbb{Z}_2 and \mathbb{Z}_3 Laplacian models on the extended square, triangular and honeycomb lattices respectively. Anisotropic models have rigid string operators along the z -direction, so they always host z -lineons. These include the fractal spin liquid [27, 46], some members of the cubic code (CC) family [5] (CC_{5,6,9}, CC₁₁₋₁₇) and the anisotropic Laplacian model [1]. Thus, they are invariant under the ER along the z -direction [32]. Therefore, in the following discussions, we will focus only on the ER of the Laplacian models living on the base 2D lattices. The ER of anisotropic Laplacian models can be obtained by anisotropic extension (de-

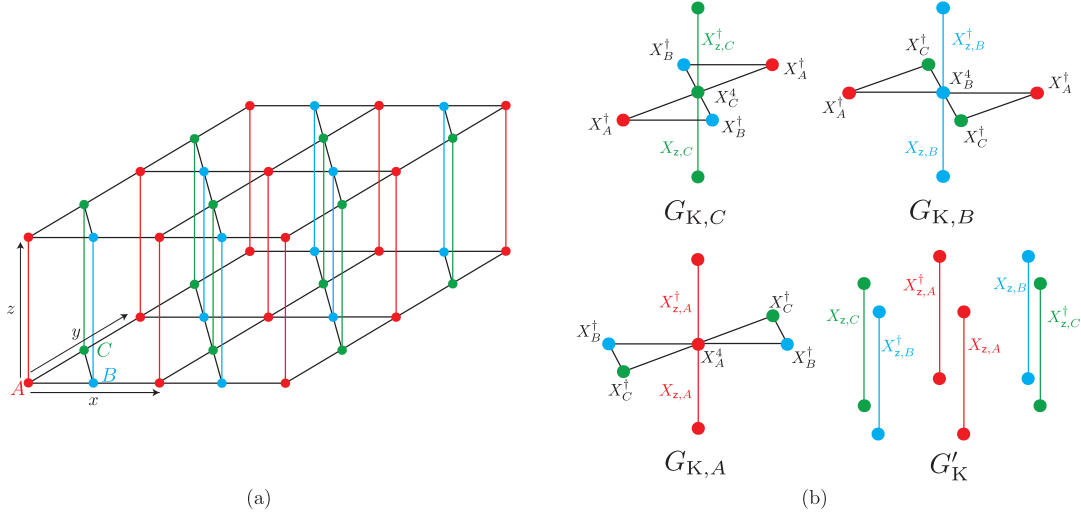


FIG. 7. (a) The prismatic lattice $\Gamma \times C_{L_z}$ with Kagome-lattice base with periodic boundary conditions. There are three sublattices denoted as red (A), blue (B) and green (C) dots respectively. (b) $G_{K,A}$, $G_{K,B}$, and $G_{K,C}$ are the stabilizer generators of the Kagome-based anisotropic Laplacian model (we do not show the F terms). When N is a multiple of 2 or 3, this model is not robust. Relatedly, there is an additional local term G'_{K} (shown for $N = 2, 3$) that acts nontrivially on the ground-state subspace and commutes with all the terms of the Hamiltonian.

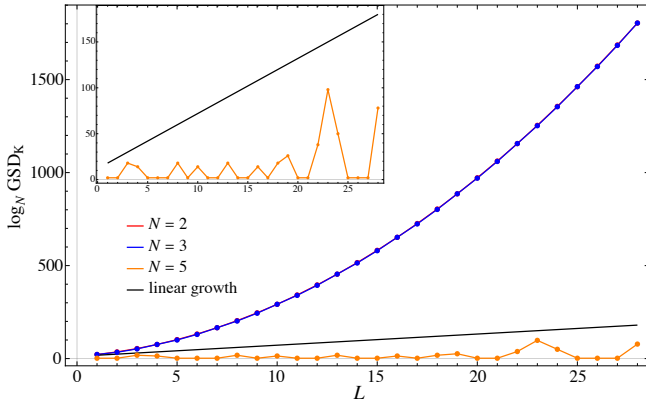


FIG. 8. The logarithm of the ground-state degeneracy of the Kagome-based anisotropic Laplacian model on the $L \times L \times L_z$ lattice with $3 \leq L \leq 30$ for $N = 2$ (red), 3 (blue), and 5 (orange). The blue line is almost on top of the red one, so the latter is not visible. The black line shows a linear function of L . The $\mathbb{Z}_{2,3}$ model is not robust as indicated by the faster-than-linear growth of $\log_{2,3} \text{GSD}$ with L . The \mathbb{Z}_5 model is robust as suggested by the at-most-linear behaviour of $\log_5 \text{GSD}$ with the system size.

scribed in Sec. II C) of all the models involved in the ER. All models are placed on an infinite lattice for the purpose of ER calculations. The explicit calculations can be found in the Mathematica file attached to this submission.

All models studied in this paper turn out to be bifurcating under an appropriate coarse-graining factor. We investigate the relationships between the GSDs before and after ER as a consistency check. We place the models on finite lattice with periodic boundary conditions to compute the GSDs. For convenience, in the following, we denote the original models as \mathcal{A} codes and the associated child models after the ER as \mathcal{B}

codes.

Throughout this paper, we will use the notation

$$H(a) \xrightarrow{c \times c} H_1(a_1) + H_2(a_2) + \dots \quad (42)$$

to denote the ER flow where the model H with the lattice spacing a flows into the models H_1, H_2, \dots with the lattice spacing ca respectively, under the coarse-graining by c along x and y directions.

A. Entanglement renormalization

The basic idea of entanglement renormalization transformation is to disentangle the short-range degrees of freedom by applying local unitary transformations [11, 12, 20, 32]. The general procedure shown in (1) consists of the following steps: (i) coarse-grain the lattice by enlarging the unit cell by the factor $c > 1$, (ii) apply local unitary transformations defined in Sec. II B, and (iii) factor out the disentangled trivial qudits.

Coarse-graining is an operation that groups sites together to form a larger unit cell [47]. In D dimensions, coarse-graining in all directions by a factor of c will enlarge the number of qudits per site and the number of stabilizer generators per site by a factor of c^D . In the polynomial language, under the coarse-graining by c in x direction while keeping the other directions the same, the polynomials in the stabilizer matrix transform as

$$x \mapsto \begin{pmatrix} 0 & x' \\ \mathbf{1}_{c-1} & 0 \end{pmatrix}, \quad y \mapsto y \mathbf{1}_c, \quad z \mapsto z \mathbf{1}_c, \quad (43)$$

where $x' = x^c$ is the new variable in the x direction.

Typically, type-II fracton models are bifurcating fixed

points only for certain values of the coarse-graining factor c . This is in contrast to ordinary topologically-ordered models and type-I fracton models, which are bifurcating fixed points for any choice of c .

B. On the square lattice

Let us first consider the \mathbb{Z}_2 Laplacian model defined on the 2D square lattice $\mathcal{A}_{\text{sq}}^{\mathbb{Z}_2}$. It is equivalent to the \mathbb{Z}_2 plaquette Ising model [48, 49] on the tilted lattice as shown in Fig. 9 whose anisotropic extension is called the anisotropic lineon model [26, 50]. The ER properties of the anisotropic lineon model have been studied in [26]; it was shown that the anisotropic lineon model flows to itself and a stack of toric codes if coarse grained along the x or y directions.

Since $\mathcal{A}_{\text{sq}}^{\mathbb{Z}_2}$ is mapped to 45° -tilted Ising plaquette model, coarse-graining of the former should be done along both x and y direction with the factor of 2. This can also be confirmed by calculating the charge annihilator and it is found that the annihilator is invariant under this coarse-graining. Concretely, the stabilizer matrix is given by

$$\mathcal{A}_{\text{sq}}^{\mathbb{Z}_2} = \begin{pmatrix} x + y + x^2y + xy^2 \\ 0 \end{pmatrix}. \quad (44)$$

The “coarse-grained” (but without any additional local unitary transformation) version of it is given by

$$\begin{pmatrix} y + xy & 1 + y & 0 & 0 \\ x + xy & 1 + x & 0 & 0 \\ 0 & 0 & y + xy & 1 + y \\ 0 & 0 & x + xy & 1 + x \\ 0 \end{pmatrix}. \quad (45)$$

We have not done any nontrivial operation yet—the coarse-graining step is just a redefinition of the unit cell—but we see that $\mathcal{A}_{\text{sq}}^{\mathbb{Z}_2}$ is transformed into two copies of a “new” model given by

$$\tilde{\mathcal{A}}_{\text{sq}}^{\mathbb{Z}_2} = \begin{pmatrix} y + xy & 1 + y \\ x + xy & 1 + x \\ 0 \end{pmatrix}. \quad (46)$$

This is nothing but the \mathbb{Z}_2 plaquette Ising model on 45° -tilted square lattice. This transformation can be denoted as

$$\mathcal{A}_{\text{sq}}^{\mathbb{Z}_2}(a) = 2 \times \tilde{\mathcal{A}}_{\text{sq}}^{\mathbb{Z}_2}(2a), \quad (47)$$

where we use $=$ to imply no qubits are dropped. Eq. (47) simply reveals that there are two copies of the plaquette Ising model on the two sublattices shown in Fig. 9.

Next, the ER transformation of $\tilde{\mathcal{A}}_{\text{sq}}^{\mathbb{Z}_2}$ is given by

$$\tilde{\mathcal{A}}_{\text{sq}}^{\mathbb{Z}_2}(a) \xrightarrow{2 \times 2} \tilde{\mathcal{A}}_{\text{sq}}^{\mathbb{Z}_2}(2a) + \text{Is}_{1+xy}^{\mathbb{Z}_2}(2a) + \text{Is}_{x+y}^{\mathbb{Z}_2}(2a), \quad (48)$$

where $\text{Is}_{1+xy}^{\mathbb{Z}_2} = (1 + xy, 0)^\top$ is a stack of 1D Ising models extended along the $(1, 1)$ direction and stacked along the $(1, -1)$ direction, and similar comments apply to $\text{Is}_{x+y}^{\mathbb{Z}_2} = (x + y, 0)^\top$. Combining (47) and (48), we have

$$\begin{aligned} \mathcal{A}_{\text{sq}}^{\mathbb{Z}_2}(a) &\xrightarrow{4 \times 4} 2\tilde{\mathcal{A}}_{\text{sq}}^{\mathbb{Z}_2}(4a) + 2(\text{Is}_{1+xy}^{\mathbb{Z}_2} + \text{Is}_{x+y}^{\mathbb{Z}_2})(4a) \\ &= \mathcal{A}_{\text{sq}}^{\mathbb{Z}_2}(2a) + 2(\text{Is}_{1+xy}^{\mathbb{Z}_2} + \text{Is}_{x+y}^{\mathbb{Z}_2})(4a) \end{aligned} \quad (49)$$

Hence, the \mathbb{Z}_2 Laplacian model on the square lattice is a quotient bifurcating fixed point. Applying the anisotropic extension along the z direction, the anisotropic \mathbb{Z}_2 Laplacian model bifurcates into itself and stacks of 2D toric codes.

The bifurcating results above can be verified by comparing the ground-state degeneracies. In the following, we use k to denote $\log_N \text{GSD}$. As reviewed in (A2), the logarithm of GSD of the \mathbb{Z}_2 Laplacian model on the square lattice with $L_x = L_y = L$ is $2L$ for even L . Therefore, the GSDs satisfy

$$k_{\mathcal{A}, \text{sq}}^{\mathbb{Z}_2}(4L) = k_{\mathcal{A}, \text{sq}}^{\mathbb{Z}_2}(2L) + 2[k_{1+xy}^{\mathbb{Z}_2}(L) + k_{x+y}^{\mathbb{Z}_2}(L)]. \quad (50)$$

This is consistent with the ER flow (49) because

$$k_{1+xy}^{\mathbb{Z}_2}(L) = k_{x+y}^{\mathbb{Z}_2}(L) = L \times k_{\text{Is}}^{\mathbb{Z}_2} = L. \quad (51)$$

Now we consider the \mathbb{Z}_3 Laplacian model on the square lattice. The stabilizer matrix is given by

$$\mathcal{A}_{\text{sq}}^{\mathbb{Z}_3} = \begin{pmatrix} xy - x^2y - xy^2 - x - y \\ 0 \end{pmatrix}. \quad (52)$$

We show that the \mathbb{Z}_3 Laplacian model is also a quotient bifurcating fixed point under the coarse-graining by 3 with the ER flow

$$\mathcal{A}_{\text{sq}}^{\mathbb{Z}_3}(a) \xrightarrow{3 \times 3} \mathcal{A}_{\text{sq}}^{\mathbb{Z}_3}(3a) + 2\mathcal{B}_{\text{sq}}^{\mathbb{Z}_3}(3a), \quad (53)$$

where

$$\mathcal{B}_{\text{sq}}^{\mathbb{Z}_3} = \begin{pmatrix} -x + y & 1 - x \\ -y + xy & 1 - xy \\ 0 \end{pmatrix}. \quad (54)$$

Under the same coarse-graining factor, the \mathcal{B} code is a self-bifurcating fixed point, i.e.

$$\mathcal{B}_{\text{sq}}^{\mathbb{Z}_3}(a) \xrightarrow{3 \times 3} 3\mathcal{B}_{\text{sq}}^{\mathbb{Z}_3}(3a). \quad (55)$$

As a consistency check, we compute the ground-state degeneracy of the \mathcal{B} code using the Gröbner basis technique for some special values of L_x and L_y (see Appendix B 4 for de-

tails). It is given by

$$k_{\mathcal{B},\text{sq}}^{\mathbb{Z}_3} = 2 \times 3^{\min(k_x, k_y)}, \quad (56)$$

where k_x and k_y are defined as in (33). For these special values of L_x and L_y , it is easy to check that

$$k_{\mathcal{A},\text{sq}}^{\mathbb{Z}_3}(3L_x, 3L_y) = k_{\mathcal{A},\text{sq}}^{\mathbb{Z}_3}(L_x, L_y) + 2k_{\mathcal{B},\text{sq}}^{\mathbb{Z}_3}(L_x, L_y), \quad (57)$$

and

$$k_{\mathcal{B},\text{sq}}^{\mathbb{Z}_3}(3L_x, 3L_y) = 3k_{\mathcal{B},\text{sq}}^{\mathbb{Z}_3}(L_x, L_y), \quad (58)$$

which are consistent with the ER flows (53) and (55), respectively.

C. On the triangular and honeycomb lattice

Next we move on to the triangular Laplacian model. Again, we first consider the \mathbb{Z}_2 case. The \mathbb{Z}_2 triangular Laplacian model is given by the stabilizer matrix

$$\mathcal{A}_{\text{tri}}^{\mathbb{Z}_2} = \begin{pmatrix} x^2y + xy^2 + x + y + x^2 + y^2 \\ 0 \end{pmatrix}. \quad (59)$$

We first coarse-grain the model along x and y directions by 2 and then apply local unitary transformations. As in (47), it leads to two “new” models,

$$\mathcal{A}_{\text{tri}}^{\mathbb{Z}_2}(a) = \tilde{\mathcal{A}}_{1,\text{tri}}^{\mathbb{Z}_2}(2a) + \tilde{\mathcal{A}}_{2,\text{tri}}^{\mathbb{Z}_2}(2a), \quad (60)$$

where $=$ again means that we do not drop any disentangled qubits. The two new models are described by the stabilizer matrices

$$\begin{aligned} \tilde{\mathcal{A}}_{1,\text{tri}}^{\mathbb{Z}_2} &= \begin{pmatrix} x + y & 0 \\ x + xy & 1 + x + y + xy \\ 0 \end{pmatrix}, \\ \tilde{\mathcal{A}}_{2,\text{tri}}^{\mathbb{Z}_2} &= \begin{pmatrix} x + y & x + xy \\ 0 & 1 + x + y + xy \\ 0 \end{pmatrix}. \end{aligned} \quad (61)$$

Furthermore, $\tilde{\mathcal{A}}_{i,\text{tri}}^{\mathbb{Z}_2}$ for $i = 1, 2$ is a quotient bifurcating fixed point. Explicitly,

$$\tilde{\mathcal{A}}_{i,\text{tri}}^{\mathbb{Z}_2}(a) \xrightarrow{2 \times 2} (\tilde{\mathcal{A}}_{i,\text{tri}}^{\mathbb{Z}_2} + \text{Is}_{1+x}^{\mathbb{Z}_2} + \text{Is}_{1+y}^{\mathbb{Z}_2} + \text{Is}_{x+y}^{\mathbb{Z}_2})(2a), \quad (62)$$

where $i = 1, 2$ and $\text{Is}^{\mathbb{Z}_2}$ represents a stack of 1D Ising models as in (48). The result resembles that of the \mathbb{Z}_2 square Laplacian model. Again, combining (60) and (62), we identify that the \mathbb{Z}_2 triangular Laplacian model is a quotient bifurcating

fixed point with the ER flow

$$\mathcal{A}_{\text{tri}}^{\mathbb{Z}_2}(a) \xrightarrow{4 \times 4} \mathcal{A}_{\text{tri}}^{\mathbb{Z}_2}(2a) + 2(\text{Is}_x^{\mathbb{Z}_2} + \text{Is}_y^{\mathbb{Z}_2} + \text{Is}_{x+y}^{\mathbb{Z}_2})(4a). \quad (63)$$

After the anisotropic extension, we identify that the \mathbb{Z}_2 triangular Laplacian models bifurcates into itself and stacks of toric codes.

Again, we compare the GSDs of the models on both sides. Recall that the GSD of the \mathbb{Z}_2 triangular Laplacian model is given by (32) (except for the factor of 2, which came from anisotropic extension). It is easy to check that

$$k_{\text{tri}}^{\mathbb{Z}_2}(4L_x, 4L_y) = k_{\text{tri}}^{\mathbb{Z}_2}(2L_x, 2L_y) + 2k_x^{\mathbb{Z}_2}(L_x, L_y) + 2k_y^{\mathbb{Z}_2}(L_x, L_y) + 2k_{x+y}^{\mathbb{Z}_2}(L_x, L_y) \quad (64)$$

where the number of 1D Ising models in the stack described by $\text{Is}_{x+y}^{\mathbb{Z}_2}$ is $\gcd(L_x, L_y)$. This is consistent with the ER flow (63).

When $N = 3$, the stabilizer matrix takes the same form as (59) but the coefficients should be understood as modulo 3. Similarly, the model seems non-bifurcating at first glance:

$$\mathcal{A}_{\text{tri}}^{\mathbb{Z}_3}(a) \xrightarrow{3 \times 3} \text{FSL}^{\mathbb{Z}_3}(3a) + \overline{\text{FSL}}^{\mathbb{Z}_3}(3a) + 2\tilde{\mathcal{A}}_{\text{tri}}^{\mathbb{Z}_3}(3a), \quad (65)$$

where $\text{FSL}^{\mathbb{Z}_3} = (1 + x + y, 0)^T$ is the \mathbb{Z}_3 fractal spin liquid, whose anisotropic extension was discussed in (37), and

$$\tilde{\mathcal{A}}_{\text{tri}}^{\mathbb{Z}_3} = \begin{pmatrix} 1 + x + y & 0 \\ 1 - y & x + y + xy \\ 0 \end{pmatrix}, \quad (66)$$

is a “new” model, analogous to (46) and (61). One step forward, we show that the ERG flow of $\tilde{\mathcal{A}}_{\text{tri}}^{\mathbb{Z}_3}$ is

$$\tilde{\mathcal{A}}_{\text{tri}}^{\mathbb{Z}_3}(a) \xrightarrow{3 \times 3} \tilde{\mathcal{A}}_{\text{tri}}^{\mathbb{Z}_3}(3a) + 2(\text{FSL}^{\mathbb{Z}_3} + \overline{\text{FSL}}^{\mathbb{Z}_3})(3a). \quad (67)$$

And the \mathbb{Z}_3 fractal spin liquid is a self-bifurcating fixed point:

$$\text{FSL}^{\mathbb{Z}_3}(a) \xrightarrow{3 \times 3} 3\text{FSL}^{\mathbb{Z}_3}(3a). \quad (68)$$

Following the same recipe as the \mathbb{Z}_2 Laplacian model on the square and triangular lattices, we find that the triangular \mathbb{Z}_3 Laplacian model is a quotient bifurcating fixed point by substituting (67) and (68) into (65), i.e.,

$$\mathcal{A}_{\text{tri}}^{\mathbb{Z}_3}(a) \xrightarrow{9 \times 9} \mathcal{A}_{\text{tri}}^{\mathbb{Z}_3}(3a) + 6(\text{FSL}^{\mathbb{Z}_3} + \overline{\text{FSL}}^{\mathbb{Z}_3})(9a). \quad (69)$$

Let us verify this ERG flow by comparing the GSDs on both sides. The GSD of the \mathbb{Z}_3 fractal spin liquid is given by $k_{\text{FSL}}^{\mathbb{Z}_3} = 3^{\min(k_x, k_y)}$, where k_x and k_y are defined as in (33) (see Appendix B 3 for details). Therefore, for these special values of L_x and L_y , we have

$$k_{\text{tri}}^{\mathbb{Z}_3}(9L_x, 9L_y) = k_{\text{tri}}^{\mathbb{Z}_3}(3L_x, 3L_y) + 6k_{\text{FSL}}^{\mathbb{Z}_3}(L_x, L_y) + 6k_{\overline{\text{FSL}}}^{\mathbb{Z}_3}(L_x, L_y), \quad (70)$$

which agrees with the ERG flow (69).

Since the honeycomb Laplacian model equals to the triangular Laplacian model when $N = 2$ and two copies of the fractal spin liquid when $N = 3$, we can straightforwardly infer the ER of the honeycomb Laplacian model from the results above.

V. DISCUSSION AND OUTLOOK

In this paper, we analyzed representative examples of anisotropic \mathbb{Z}_N Laplacian models, defined on anisotropic extensions of various 2D regular lattices. Similar to the square lattice case [1], we found the scaling behaviour of the GSD and the mobility of point-like excitations to depend sensitively on the value of N . In addition, many features of fracton phases are, not surprisingly, sensitive to lattice geometries. For example, the Kagome-based anisotropic $\mathbb{Z}_{2,3}$ Laplacian model is not robust while those based on the square, triangular, and honeycomb lattices are. Moreover, the entanglement renormalization group flows also varies with geometries: the anisotropic $\mathbb{Z}_{2,3}$ square-based and triangular-based Laplacian models are quotient bifurcating fixed points, whereas the anisotropic \mathbb{Z}_3 honeycomb Laplacian model is self-bifurcating. Incidentally, we also showed that the triangular-based and honeycomb-based models are equivalent when N is not a multiple of 3.

We remark that the ER property can be sensitive to coarse-graining factors. Let us first consider the stabilizer models hosting string operators. This includes topological quantum liquid phases such the 2D or 3D toric code, foliated fracton order, and any anisotropic extension of a classical model, such as the anisotropic Laplacian model. (As explained before, the anisotropic extension necessarily hosts string operators along the anisotropic direction, but it is model-dependent in the other directions.) The topological quantum liquid phases are scale-invariant, thus are fixed points under the ER with arbitrary integer c [12, 14]. Similarly, fracton models that can be constructed by coupled layers are bifurcating for any c when coarse-grained along the direction perpendicular to those layers. For example, we can coarse-grain the X-cube model by a factor of 3 along x direction and the resulting Hamiltonian is equivalent to the X-cube model plus two stacks of 2D toric codes on the yz planes. However, for models discussed in this paper, which do not host string operators within the xy plane, we should be careful about the choice of coarse-graining factors, similar to Haah's cubic codes $CC_{1-4,7,8,10}$.

There are several immediate questions that arise from this work. It would be interesting to systematically work out the entanglement renormalization flow of Laplacian models for arbitrary N . While a rigorous proof is lacking, an example for $N = 5$ shows similar bifurcating behaviors as that of the $N = 2, 3$ case, indicating that the ER captures universal features of fracton phases. When N is composite, we expect that under ER, more elementary $\mathbb{Z}_{\tilde{N}}$ models will further be generated where $N = c\tilde{N}$ with $c > 1$ is an integer. The current approaches in this work rely on techniques from commutative algebra and are most useful when N is prime. We leave a

more systematic examination of the general cases for future work.

A more general question in the context of ER is determining when a model is a bifurcating fixed point. In the case of $\mathbb{Z}_{2,3}$ Laplacian models, we have shown that the model is reproduced under ER when the coarse-graining factor is chosen to be $c = 2$ or 3 , respectively, in both x and y directions. This suggests that the \mathbb{Z}_p Laplacian model is bifurcating under ER when coarse-grained by $c = p$. In fact, we believe that the same is true for any stabilizer code based on qudits of prime dimension p . It would be nice to confirm this intuition, perhaps using techniques from commutative algebra. We leave the resolution of these questions to future work.

We also believe that the study of ER can be generalized to a broader range of fracton order such as the fermionic fracton order [51–53], but we leave a careful study of these models to the future. Lastly, we remark that complementary tensor network methods such as MERAs [35] and TEFRs [54] which are more focused on states can also be helpful in understanding the renormalization properties of fracton phases.

ACKNOWLEDGMENTS

We thank Daniel Bulmash, Meng Cheng, Arpit Dua, Ho Tat Lam, Shu-Heng Shao, and Nathanan Tantivasadakarn for helpful discussions. Z.-X. L. is grateful to Andreas Karch and Hao-Yu Sun for their hospitality at UT Austin. Y. X. is supported by the National Science Foundation under NSF Award Number DMR – 2308817. P. G. is supported by the Simons Collaboration on Global Categorical Symmetries. Z.-X. L. is partially supported by the Simons Collaborations on Ultra-Quantum Matter, grant 651440 from the Simons Foundation.

Appendix A: Review of anisotropic \mathbb{Z}_N Laplacian model on the square lattice

In this appendix, we review the 3+1D \mathbb{Z}_N anisotropic Laplacian model on an $L_x \times L_y \times L_z$ cubic lattice with periodic boundary conditions in all three directions [1]. The graph Γ is taken to be a torus $C_{L_x} \times C_{L_y}$. The stabilizer matrix of the corresponding (classical) Laplacian model is $(f, 0)^T$, where

$$f(x, y) = x(y - 1)^2 + y(x - 1)^2 \pmod{N}. \quad (\text{A1})$$

When $N = 2$, assuming L_x, L_y are both even or infinite, the square-based anisotropic Laplacian model is equivalent to two copies of the 3+1D anisotropic \mathbb{Z}_2 lineon model [26, 50] defined on a 45° tilted square lattice [1] shown in Fig. 9. The logarithm of the GSD for $L_x = L_y = L$ is given by

$$\log_2 \text{GSD}_{\text{sq}} = \begin{cases} 4L, & L \text{ is even,} \\ 4L - 2, & L \text{ is odd.} \end{cases} \quad (\text{A2})$$

When $N = p > 2$ is an odd prime, things become significantly different. In this case, let $q \neq p$ be another odd prime such that p is a primitive root modulo q^m with integer $m \geq 1$.

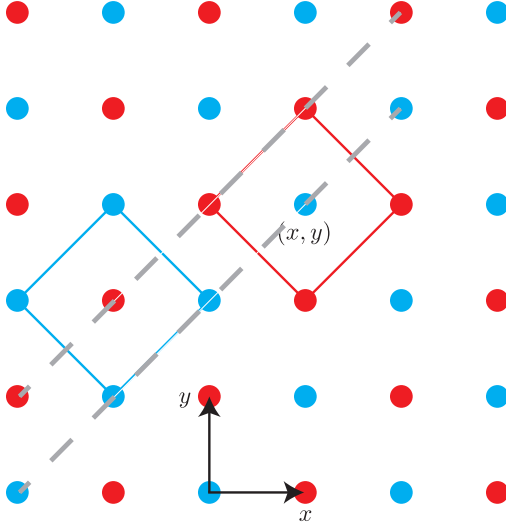


FIG. 9. The anisotropic \mathbb{Z}_2 Laplacian model is equivalent to two copies of the anisotropic \mathbb{Z}_2 lineon model on the red and blue sublattices, respectively (the z -direction is suppressed). The gray dashed lines represent the string-like logical operators in the $(1, 1)$ direction.

For $L_x = p^{k_x} q^m$ and $L_y = p^{k_y} q^m$ where $k_x, k_y, m, \geq 0$ are

integers, we have

$$\log_p \text{GSD}_{\text{sq}} = 2(2p^{\min(k_x, k_y)} - \delta_{k_x, k_y}). \quad (\text{A3})$$

Let us discuss the mobility of the excitations on the infinite lattice. The string-like logical operators in the z -direction indicate that the model has lineons which can move along z -direction. However, the mobility of the z -lineons on the xy plane is nontrivial. We will closely follow the argument in [1] and Appendix C.

For $N = 2$, $f(x, y)$ in (A1) is factorizable since $f(x, y) = (x + y)(1 + \bar{x}\bar{y}) \pmod{2}$. To satisfy the mobility condition (C2), we can take (n_0, m_0) to be $(n, \pm n)$. When $(n_0, m_0) = (n, n)$, we have the factorization

$$x^n y^n + 1 = (xy + 1)(x^{n-1} y^{n-1} + \dots + 1) \pmod{2}. \quad (\text{A4})$$

And $q(x, y)$ can be chosen as $x + y$. This is exactly the case that a dipole of z -lineons separated in the $(1, -1)$ direction can move in the $(1, 1)$. The dashed lines in Fig. 9 represent the string operators that move the dipole. On the other hand, for $(n_0, m_0) = (n, -n)$, a dipole of z -lineons separated in the $(1, 1)$ direction can move in the $(1, -1)$.

For $N = p > 2$, $f(x, y)$ is irreducible up to any monomial. Following the argument in [1], we have that $x^{n_0} y^{m_0} - 1$ is not a multiple of $f(x, y)$. Thus the condition (C2) cannot be satisfied, except trivially, and any finite set of z -lineons in the anisotropic \mathbb{Z}_p Laplacian model cannot move in the xy plane, except when they are created locally.

Appendix B: Ground-state degeneracies of the Laplacian models and the associated \mathcal{B} codes

1. General procedure

The analytical method to compute the ground-state degeneracy of translationally invariant Pauli stabilizer codes based on qudits of prime dimension p involves using the Gröbner basis to calculate the dimension of a quotient ring, or more generally a quotient module [42]⁸. For concreteness, let us work in 2D with coordinates (x, y) and periodic boundary conditions $(x, y) \sim (x + L_x, y) \sim (x, y + L_y)$. The starting point is the stabilizer map $\mathcal{A} : \mathbb{F}_p[x, y]^t \rightarrow \mathbb{F}_p[x, y]^{2q}$, which is given by the $2q \times t$ matrix defined in Sec. II. In all our applications below, it turns out that $q = t$, i.e., the number of qudits per site is equal to the number of different type of stabilizer terms. In this case, the GSD is given by

$$\log_p \text{GSD} = \dim_{\mathbb{F}_p} \text{coker } \mathcal{A}_L^\dagger = \dim_{\mathbb{F}_p} (\mathbb{F}_p[x, y]/\mathfrak{b}_L)^t / \text{im } \mathcal{A}_L^\dagger, \quad (\text{B1})$$

where, $\mathfrak{b}_L = (x^{L_x} - 1, y^{L_y} - 1)$ is the ideal that effectively imposes the periodic boundary conditions and \mathcal{A}_L is the same matrix as \mathcal{A} that acts on the quotient ring $\mathbb{F}_p[x, y]/\mathfrak{b}_L$ instead of $\mathbb{F}_p[x, y]$.

For a classical code, only the first q rows of \mathcal{A} are nonzero, so we can replace \mathcal{A}^\dagger with $(\mathcal{A}^Z)^\dagger$ in (B1). Recall that the GSDs of a classical code and its anisotropic extension are related by (21). So, in all applications below, we compute the \log_p GSD of the \mathbb{Z}_p Laplacian models and their \mathcal{B} codes, which are all classical codes. Multiplying the results by 2 gives the expressions for the GSDs of their anisotropic extensions.

⁸ While [42] considers only qubits explicitly, as stated there, all their results generalize straightforwardly to qudits of any prime dimension p .

a. Gröbner basis of ideals of polynomial rings for $q = t = 1$

In the special case of $q = t = 1$, $\text{im } \mathcal{A}^\dagger$ is simply the ideal (f) of $\mathbb{F}_p[x, y]$, where $f(x, y)$ is the nonzero entry of \mathcal{A}^9 . Therefore, the expression for GSD can be written as

$$\log_p \text{GSD} = \dim_{\mathbb{F}_p} \mathbb{F}_p[x, y]/\mathfrak{i}, \quad (\text{B2})$$

where $\mathfrak{i} = (f) + \mathfrak{b}_L = (f, x^{L_x} - 1, y^{L_y} - 1)$.

Let us briefly review the Gröbner basis technique to compute this quantity. Given an ideal \mathfrak{i} of the polynomial ring $\mathbb{F}[x, y]$, where \mathbb{F} is a field, the vector space dimension of the quotient ring $\mathbb{F}[x, y]/\mathfrak{i}$ can be computed using the Gröbner basis of \mathfrak{i} . In particular, if $\mathcal{G} = \{g_1, \dots, g_n\}$ denotes the Gröbner basis of \mathfrak{i} with respect to a monomial order¹⁰, then any polynomial $P \in \mathbb{F}[x, y]$ can be written as

$$P(x, y) = R(x, y) + \sum_{i=1}^n Q_i(x, y)g_i(x, y), \quad (\text{B3})$$

where R is not reducible with respect to \mathcal{G} ¹¹. While Q_i 's (à la quotients) may not be uniquely determined, the polynomial R (à la remainder) is uniquely determined by P . The uniqueness of R is one of the defining properties of a Gröbner basis. Therefore, we may rewrite the above equation as

$$P(x, y) = R(x, y) \pmod{\mathcal{G}}. \quad (\text{B4})$$

It follows that $\mathbb{F}[x, y]/\mathfrak{i}$ is in one-one correspondence with the set of polynomials that are irreducible with respect to \mathcal{G} . Therefore, the set of monomials that are irreducible with respect to \mathcal{G} forms a basis of the vector space $\mathbb{F}[x, y]/\mathfrak{i}$. So, computing $\dim_{\mathbb{F}} \mathbb{F}[x, y]/\mathfrak{i}$ is equivalent to counting the number of monomials that are irreducible with respect to the Gröbner basis of \mathfrak{i} .

b. Alternative expression for GSD when $q = t = 1$

While there are computer algebra systems that compute the Gröbner basis of an ideal quickly and efficiently, computing it analytically is hard. The following manipulations yield another expression for the GSD that is more amenable to analytic computation.

It is well-known that any Artinian ring¹² \mathcal{R} has a finite number of maximal ideals and has a canonical decomposition $\mathcal{R} \cong \bigoplus_{\mathfrak{m}} \mathcal{R}_{\mathfrak{m}}$, where the sum is over the maximal ideals \mathfrak{m} of \mathcal{R} and $\mathcal{R}_{\mathfrak{m}}$ denotes the localization of \mathcal{R} at \mathfrak{m} ¹³. Therefore,

$$\log_p \text{GSD} = \dim_{\mathbb{F}_p} \mathbb{F}_p[x, y]/\mathfrak{i} = \sum_{\mathfrak{m}} \dim_{\mathbb{F}_p} (\mathbb{F}_p[x, y]/\mathfrak{i})_{\mathfrak{m}}. \quad (\text{B5})$$

The maximal ideals of $\mathbb{F}_p[x, y]/\mathfrak{i}$ are related to those of $\mathbb{F}_p[x, y]$ by the following theorem:

Theorem B.1. *The maximal ideals of \mathcal{R}/\mathfrak{i} are in one-one correspondence with the maximal ideals of \mathcal{R} that contain \mathfrak{i} .*

However, the maximal ideals of $\mathbb{F}_p[x, y]$ are hard to compute in general. Instead, it is simpler to work with the algebraic closure of \mathbb{F}_p , denoted as $\overline{\mathbb{F}} = \overline{\mathbb{F}_p}$. Since the vector space dimension does not change under the extension of the underlying field, we have

$$\log_p \text{GSD} = \sum_{\mathfrak{m}} \dim_{\overline{\mathbb{F}}} (\overline{\mathbb{F}}[x, y]/\mathfrak{i})_{\mathfrak{m}}, \quad (\text{B6})$$

where \mathfrak{i} is now interpreted as the ideal of $\overline{\mathbb{F}}[x, y]$ generated by the same polynomials as before.

The simplicity of working with algebraic closure stems from the following theorem:

⁹ More precisely, $\text{im } \mathcal{A}^\dagger$ is the ideal (\bar{f}) , but in our application, $\bar{f}(x, y) = f(\bar{x}, \bar{y}) = \bar{x}^2 \bar{y}^2 f(x, y)$ which is equivalent to $f(x, y)$ up to a monomial (i.e., translations).

¹⁰ We always use the lexicographic monomial order $x \succ y$ in computing the Gröbner basis.

¹¹ A polynomial P is reducible with respect to a set of polynomials $\{g_1, \dots, g_n\}$ if the leading term of P is a multiple of the leading term of one of the g_i 's. Here, the leading term of a polynomial is defined with respect to the monomial order.

¹² An Artinian ring is a ring that satisfies the descending chain condition, i.e., if $\mathfrak{i}_1 \supseteq \mathfrak{i}_2 \supseteq \dots$ is a descending chain of ideals, then there is a $k \geq 1$ such that $\mathfrak{i}_k = \mathfrak{i}_{k+1} = \dots$. Any ring that is a finite dimensional vector space over a field is always Artinian, which is exactly the case here.

¹³ The idea behind localization is to “put in by hand” multiplicative inverses of some elements in a ring \mathcal{R} . More precisely, the localization of \mathcal{R} with respect to a multiplicatively closed set S is a new ring, denoted as $S^{-1}\mathcal{R}$, whose elements are fractions with numerators in \mathcal{R} and denominators in S . Given a maximal ideal \mathfrak{m} of a ring \mathcal{R} , $\mathcal{R} \setminus \mathfrak{m}$ is always multiplicatively closed. We define the localization of \mathcal{R} at \mathfrak{m} , denoted as $\mathcal{R}_{\mathfrak{m}}$, as the localization of \mathcal{R} with respect to $\mathcal{R} \setminus \mathfrak{m}$.

Theorem B.2 (Weak form of Hilbert's Nullstellensatz). *Let \mathbb{F} be an algebraically closed field. The maximal ideals of the polynomial ring $\mathbb{F}[x_1, \dots, x_n]$ are of the form $(x_1 - a_1, \dots, x_n - a_n)$ for some $a_i \in \mathbb{F}$.*

The maximal ideals of $\mathbb{F}[x, y]$ are therefore of the form $(x - x_0, y - y_0)$ for some $x_0, y_0 \in \mathbb{F}$. The ideal $(x - x_0, y - y_0)$ contains \mathfrak{i} if and only if (x_0, y_0) is a root of all polynomials in \mathfrak{i} . Hence,

$$\log_p \text{GSD} = \sum_{(x_0, y_0) \in V(\mathfrak{i})} \dim_{\mathbb{F}}(\mathbb{F}[x, y]/\mathfrak{i})_{(x-x_0, y-y_0)}, \quad (\text{B7})$$

where

$$V(\mathfrak{i}) = \{(x, y) \in \mathbb{F}^2 : f(x, y) = x^{L_x} - 1 = y^{L_y} - 1 = 0\}. \quad (\text{B8})$$

To further simplify the calculations, let $L_i = p^{k_i} L'_i$ with $p \nmid L'_i$ ¹⁴. Then we have the factorization,

$$\begin{aligned} x^{L_x} - 1 &= x^{L_x} - x_0^{L_x} = (x^{L'_x})^{p^{k_x}} - (x_0^{L'_x})^{p^{k_x}} = (x^{L'_x} - x_0^{L'_x})^{p^{k_x}} \\ &= (x - x_0)^{p^{k_x}} (x^{L'_x-1} + x^{L'_x-2} x_0 + \dots + x_0^{L'_x-1})^{p^{k_x}}, \end{aligned} \quad (\text{B9})$$

and similarly for $y^{L_y} - 1$. The polynomial in the second bracket of the second line is a unit¹⁵ in the localization $\mathbb{F}[x, y]_{(x-x_0, y-y_0)}$. Therefore, $(x^{L_x} - 1, y^{L_y} - 1)$ generates the same ideal as $((x - x_0)^{p^{k_x}}, (y - y_0)^{p^{k_y}})$ in $\mathbb{F}[x, y]_{(x-x_0, y-y_0)}$. Defining

$$\mathfrak{i}_{x_0, y_0} = (f, (x - x_0)^{p^{k_x}}, (y - y_0)^{p^{k_y}}), \quad (\text{B10})$$

the quotient ring becomes¹⁶

$$\begin{aligned} (\mathbb{F}[x, y]/\mathfrak{i})_{(x-x_0, y-y_0)} &\cong \mathbb{F}[x, y]_{(x-x_0, y-y_0)} / \mathfrak{i}_{(x-x_0, y-y_0)} \\ &\cong \mathbb{F}[x, y]_{(x-x_0, y-y_0)} / (\mathfrak{i}_{x_0, y_0})_{(x-x_0, y-y_0)} \\ &\cong (\mathbb{F}[x, y]/\mathfrak{i}_{x_0, y_0})_{(x-x_0, y-y_0)}. \end{aligned} \quad (\text{B11})$$

In the first and third lines, we used the fact that localization commutes with quotient. Note that the quotient ring $\mathbb{F}[x, y]/\mathfrak{i}_{x_0, y_0}$ is also Artinian, and by Hilbert's Nullstellensatz, its only maximal ideal is $(x - x_0, y - y_0)$. Therefore,

$$(\mathbb{F}[x, y]/\mathfrak{i}_{x_0, y_0})_{(x-x_0, y-y_0)} \cong \mathbb{F}[x, y]/\mathfrak{i}_{x_0, y_0}, \quad (\text{B12})$$

and hence,

$$\log_p \text{GSD} = \sum_{(x_0, y_0) \in V(\mathfrak{i})} \dim_{\mathbb{F}} \mathbb{F}[x, y]/\mathfrak{i}_{x_0, y_0}. \quad (\text{B13})$$

This is the desired alternative expression for the GSD.

c. Gröbner basis of submodules of free modules for $q = t > 1$

When $q = t > 1$, $\text{im } \mathcal{A}^\dagger$ is not an ideal of $\mathbb{F}_p[x, y]$. Instead, it is a submodule of the free module $\mathbb{F}_p[x, y]^t$. The above Gröbner basis techniques generalize straightforwardly to this case. Let us briefly introduce the Gröbner basis of a submodule of a free module [55].

Let $\mathcal{R} = \mathbb{F}[x, y]$ be a polynomial ring over a field \mathbb{F} . Then, the Cartesian product

$$\mathcal{R}^t = \{\mathbf{f} = (f_1, \dots, f_t)^\top : f_i \in \mathcal{R}, i = 1, \dots, t\}, \quad (\text{B14})$$

is a free \mathcal{R} -module of rank t , i.e., it has a linearly independent finite generating set (i.e., a basis) of size t given by

$$\mathbf{e}_1 = (1, 0, \dots, 0)^\top, \quad \dots, \quad \mathbf{e}_t = (0, \dots, 0, 1)^\top. \quad (\text{B15})$$

¹⁴ $a \nmid b$ means a does not divide b .

¹⁵ A unit is an element of the ring with a multiplicative inverse, i.e., u is a unit if there exists v in the ring such that $uv = 1$.

¹⁶ Given an ideal \mathfrak{i} of a ring \mathcal{R} , the ideal \mathfrak{i}_m of \mathcal{R}_m is generated by the image of \mathfrak{i} under the localization map $\mathcal{R} \rightarrow \mathcal{R}_m$.

A submodule \mathcal{M} of \mathcal{R}^t is a subset that satisfies $r \cdot \mathbf{f} \in \mathcal{M}$ for any $r \in \mathcal{R}$ and $\mathbf{f} \in \mathcal{M}$. For example, given a $t \times s$ matrix $\tau : \mathcal{R}^s \rightarrow \mathcal{R}^t$, its image $\text{im } \tau$ is a submodule of \mathcal{R}^t generated by the columns of τ . Note that this submodule is not necessarily a free \mathcal{R} -module, even though it has finitely many (s) generators because they can have nontrivial relations (known as “syzygies”) among them.

A monomial of \mathcal{R}^t is defined as a monomial of \mathcal{R} times a basis vector, i.e., $x^a y^b \mathbf{e}_i$ for some nonnegative integers a, b and $i = 1, \dots, t$. We say a monomial $x^a y^b \mathbf{e}_i$ is a multiple of another monomial $x^c y^d \mathbf{e}_j$ if $i = j$, $a \geq c$, and $b \geq d$. We define $\text{lcm}(x^a y^b \mathbf{e}_i, x^c y^d \mathbf{e}_j) = x^{\max(a,c)} y^{\max(b,d)} \mathbf{e}_i$ if $i = j$ and 0 otherwise.

Given a monomial order on \mathcal{R} , such as the lexicographic monomial order $x \succ y$, one can define several natural monomial orders on \mathcal{R}^t . The one we will use is the “term over position” (TOP) order, where

$$x^a y^b \mathbf{e}_i \succ x^c y^d \mathbf{e}_j \iff x^a y^b \succ x^c y^d, \quad \text{or} \quad x^a y^b = x^c y^d \text{ and } i > j. \quad (\text{B16})$$

The leading term of $\mathbf{f} \in \mathcal{R}^t$, denoted as $\text{lt}(\mathbf{f})$, is the largest term in \mathbf{f} with respect to the monomial order. For any nonempty subset S of \mathcal{R}^t , we define $\text{lt}(S)$ as the submodule of \mathcal{R}^t generated by the leading terms of the elements of S .

We now give the definition of the Gröbner basis for a submodule of a free \mathcal{R} -module [55], which is quite similar to that of an ideal of \mathcal{R} .

Definition B.1. Let $\mathcal{M} \neq 0$ be a submodule of \mathcal{R}^t and \mathcal{G} be a finite subset of \mathcal{M} . Then \mathcal{G} is a Gröbner basis of \mathcal{M} if $\text{lt}(\mathcal{M}) = \text{lt}(\mathcal{G})$.

Theorem B.3. Let $\mathcal{M} \neq 0$ be a submodule of \mathcal{R}^t and $\mathcal{G} = \{\mathbf{g}_1, \dots, \mathbf{g}_n\}$ be a finite subset of nonzero vectors of \mathcal{M} . Then the following are equivalent:

- (i) \mathcal{G} is a Gröbner basis of \mathcal{M} .
- (ii) For any vector $\mathbf{f} \in \mathcal{R}^t$, $\mathbf{f} \in \mathcal{M} \iff \mathbf{f}$ can be reduced to $\mathbf{0}$ by \mathcal{G} .¹⁷
- (iii) For any vector $\mathbf{f} \in \mathcal{M}$, there exists polynomials $q_1, \dots, q_n \in \mathcal{R}$ such that

$$\mathbf{f} = \sum_{i=1}^n q_i \mathbf{g}_i.$$

Similar to the case of a quotient ring, the quotient module $\mathcal{R}^t/\mathcal{M}$ is a set of equivalence classes, each of which is represented by a vector in \mathcal{R}^t that is irreducible with respect to the Gröbner basis \mathcal{G} of \mathcal{M} . Therefore, the vector-space dimension of the quotient module, $\dim_{\mathbb{F}}(\mathcal{R}^t/\mathcal{M})$, is equal to the number of monomials of \mathcal{R}^t that are irreducible with respect to \mathcal{G} .

d. Alternative expression for GSD when $q = t > 1$

As in the case of ideals, computing the Gröbner basis of submodules of free modules over $\mathbb{F}_p[x, y]$ analytically is very hard. So, once again, we perform the following manipulations to get another expression for the GSD that is more tractable analytically.

The first step is to localize the module at the maximal ideals of $\mathbb{F}_p[x, y]$. Say \mathcal{R} is an Artinian ring, which means it has a finite number of maximal ideals and satisfies $\mathcal{R} \cong \bigoplus_{\mathfrak{m}} \mathcal{R}_{\mathfrak{m}}$. Then, any finitely generated \mathcal{R} -module \mathcal{M} satisfies $\mathcal{M} \cong \bigoplus_{\mathfrak{m}} \mathcal{M}_{\mathfrak{m}}$ ¹⁸, where $\mathcal{M}_{\mathfrak{m}}$ denotes the localization of \mathcal{M} at \mathfrak{m} . Moreover, $\mathcal{M}_{\mathfrak{m}}$ is nonzero if and only if \mathfrak{m} contains the zeroth Fitting ideal of \mathcal{M} . If $\tau : \mathcal{R}^s \rightarrow \mathcal{R}^t$ is a $t \times s$ matrix, then the k -th Fitting ideal of $\mathcal{M} = \text{coker } \tau$ is the ideal generated by the $(t - k) \times (t - k)$ minors of τ . Using these facts for $\mathcal{R} = \mathbb{F}_p[x, y]/\mathfrak{b}_L$ and $\tau = \mathcal{A}^\dagger$, the GSD is given by

$$\log_p \text{GSD} = \sum_{\mathfrak{m} \supseteq (f)} \dim_{\mathbb{F}_p}[(\mathbb{F}_p[x, y]/\mathfrak{b}_L)^t / \text{im } \mathcal{A}^\dagger]_{\mathfrak{m}}, \quad (\text{B17})$$

where $f(x, y) = \det(\mathcal{A}^Z)^\dagger$ is the only nonzero $t \times t$ minor of \mathcal{A}^\dagger .

Next, we extend the base field from \mathbb{F}_p to its algebraic closure $\mathbb{F} = \overline{\mathbb{F}_p}$. This does not change the vector-space dimension, so

$$\log_p \text{GSD} = \sum_{\mathfrak{m} \supseteq (f)} \dim_{\mathbb{F}}[(\mathbb{F}[x, y]/\mathfrak{b}_L)^t / \text{im } \mathcal{A}^\dagger]_{\mathfrak{m}}. \quad (\text{B18})$$

¹⁷ A vector $\mathbf{f} \in \mathcal{R}^t$ is reducible with respect to a set of vectors $\{\mathbf{g}_1, \dots, \mathbf{g}_n\}$ if the leading term of \mathbf{f} is a multiple of the leading term of one of the \mathbf{g}_i 's.

¹⁸ To see this, first tensor both sides of $\mathcal{R} \cong \bigoplus_{\mathfrak{m}} \mathcal{R}_{\mathfrak{m}}$ with \mathcal{M} and then use the facts that $\mathcal{R} \otimes_{\mathcal{R}} \mathcal{M} \cong \mathcal{M}$, tensoring is right-exact, and tensoring commutes with direct sum and localization.

The maximal ideals of $\mathbb{F}[x, y]/\mathfrak{b}_L$ are in one-one correspondence with maximal ideals of $\mathbb{F}[x, y]$ that contain \mathfrak{b}_L . By Hilbert's Nullstellensatz, the maximal ideals of $\mathbb{F}[x, y]$ are of the form $(x - x_0, y - y_0)$ for some $x_0, y_0 \in \mathbb{F}$. And the ideal $(x - x_0, y - y_0)$ contains \mathfrak{i} if and only if (x_0, y_0) is a root of all the polynomials in \mathfrak{i} . Hence,

$$\log_p \text{GSD} = \sum_{(x_0, y_0) \in V(\mathfrak{i})} \dim_{\mathbb{F}}[(\mathbb{F}[x, y]/\mathfrak{b}_L)^t / \text{im } \mathcal{A}^\dagger]_{(x-x_0, y-y_0)}, \quad (\text{B19})$$

where $\mathfrak{i} = (f) + \mathfrak{b}_L$ and

$$V(\mathfrak{i}) = \{(x, y) \in \mathbb{F}^2 : f(x, y) = x^{L_x} - 1 = y^{L_y} - 1 = 0\}. \quad (\text{B20})$$

Let $L_i = p^{k_i} L'_i$, where $p \nmid L'_i$. By the same argument as before, within the localization at $(x - x_0, y - y_0)$, we can replace $x^{L_x} - 1$ with $(x - x_0)^{p^{k_x}}$ and $y^{L_y} - 1$ with $(y - y_0)^{p^{k_y}}$. That is, $\mathfrak{b}_{L; x_0, y_0} = ((x - x_0)^{p^{k_x}}, (y - y_0)^{p^{k_y}})$ is the same ideal as \mathfrak{b}_L in $\mathbb{F}[x, y]_{(x-x_0, y-y_0)}$. Therefore, we have

$$\log_p \text{GSD} = \sum_{(x_0, y_0) \in V(\mathfrak{i})} \dim_{\mathbb{F}}[(\mathbb{F}[x, y]/\mathfrak{b}_{L; x_0, y_0})^t / \text{im } \mathcal{A}^\dagger]_{(x-x_0, y-y_0)}. \quad (\text{B21})$$

Now, $\mathbb{F}[x, y]/\mathfrak{b}_{L; x_0, y_0}$ is an Artinian ring, and by Hilbert's Nullstellensatz, its only maximal ideal is $(x - x_0, y - y_0)$, so $(\mathbb{F}[x, y]/\mathfrak{b}_{L; x_0, y_0})_{(x-x_0, y-y_0)} \cong \mathbb{F}[x, y]/\mathfrak{b}_{L; x_0, y_0}$. Therefore,

$$\log_p \text{GSD} = \sum_{(x_0, y_0) \in V(\mathfrak{i})} \dim_{\mathbb{F}}(\mathbb{F}[x, y]/\mathfrak{b}_{L; x_0, y_0})^t / \text{im } \mathcal{A}^\dagger = \sum_{(x_0, y_0) \in V(\mathfrak{i})} \dim_{\mathbb{F}} \mathbb{F}[x, y]^t / \text{im } \tau_{x_0, y_0}, \quad (\text{B22})$$

where

$$\tau_{x_0, y_0} = \begin{pmatrix} \mathcal{A}^\dagger & (x - x_0)^{p^{k_x}} \mathbf{1}_t \\ & (y - y_0)^{p^{k_y}} \mathbf{1}_t \end{pmatrix}. \quad (\text{B23})$$

It is easy to check that when $q = t = 1$, this expression reduces to the one in (B13).

2. \mathbb{Z}_p Laplacian model on the triangular lattice

In this case, $q = t = 1$, so we use the alternative expression (B13) to compute the GSD of this model for some special values of L_x and L_y . The ideal we are dealing with is $\mathfrak{i} = (f, x^{L_x} - 1, y^{L_y} - 1)$ with $f(x, y) = -6xy + x + y + x^2 + y^2 + x^2y + xy^2$. Let (x_0, y_0) be the solution of the system of polynomial equations

$$f(x, y) = x^{L_x} - 1 = y^{L_y} - 1 = 0. \quad (\text{B24})$$

Under the factorization $x^{L_x} - 1 = (x^{L'_x} - 1)^{p^{k_x}}$ where $p \nmid L'_x$, it becomes

$$f(x, y) = x^{L'_x} - 1 = y^{L'_y} - 1 = 0. \quad (\text{B25})$$

Let us start from the simplest special case $L'_x = L'_y = 1$. Obviously, the only solution in this case is $(x_0, y_0) = (1, 1)$. We assume without loss of generality that $k_x \geq k_y$. The Gröbner basis for $p = 3$ and $p > 3$ are different, so we discuss them separately.

For $p = 3$, $f(x, y) = (1 + x + y)(x + y + xy)$, and the Gröbner basis is given as

$$g_1 = y^{3^{k_y} - 1} - 1, \quad g_2 = x^2 + x \sum_{i=2}^{3^{k_y} - 1} (-y)^i + y. \quad (\text{B26})$$

The set of monomials that are irreducible with respect to this Gröbner basis is

$$\{1, y, \dots, y^{3^{k_y} - 1}, x, xy, \dots, xy^{3^{k_y} - 1}\}, \quad (\text{B27})$$

with cardinality 2×3^{k_y} . By (B13), we conclude

$$\log_3 \text{GSD}_{\text{tri}} = 2 \times 3^{k_y}. \quad (\text{B28})$$

For $p > 3$, the Gröbner basis is given as follows:

(1) When $k_x \neq k_y$,

$$g_1 = y^{p^{k_y}} - 1, \quad g_2 = x^2 + 4x \sum_{i=2}^{p^{k_y}-1} (-y)^i - 3xy - 3x + y. \quad (\text{B29})$$

The set of monomials which are irreducible with respect to this Gröbner basis is

$$\{1, y, \dots, y^{p^{k_y}-1}, x, xy, \dots, xy^{p^{k_y}-1}\}, \quad (\text{B30})$$

with cardinality $2p^{k_y}$.

(2) When $k_x = k_y = k$ ¹⁹,

$$g_1 = y^{p^k} - 1, \quad g_2 = x^2 + 4x \sum_{i=2}^{p^k-1} (-y)^i - 3xy - 3x + y, \quad g_3 = (x-1) \sum_{i=0}^{p^k-1} y^i. \quad (\text{B31})$$

The set of monomials which are irreducible with respect to this Gröbner basis is

$$\{1, y, \dots, y^{p^k-1}, x, xy, \dots, xy^{p^k-2}\}, \quad (\text{B32})$$

with cardinality $2p^{k_y} - 1$.

Combining the two cases together, the number of irreducible monomials is $2p^{k_y} - \delta_{k_x, k_y}$. By (B13), we conclude

$$\log_p \text{GSD}_{\text{tri}} = 2p^{k_y} - \delta_{k_x, k_y}, \quad p > 3. \quad (\text{B33})$$

Proof of Gröbner basis. Let us work with arbitrary odd prime p , including $p = 3$, and deal with the special cases when necessary. It is easy to check that each of the above Gröbner bases satisfies the Buchberger's criterion. It is also easy to verify that

$$f = -4xg_1 + (y+1)g_2, \quad g_2 = a \left[\sum_{i=0}^{p^{k_y}-1} (-y)^i f + (x^2 + xy - 7x + y)(y^{p^{k_y}} - 1) \right], \quad (\text{B34})$$

where a is the reciprocal of 2 modulo p , i.e., a is an integer satisfying $2a \equiv 1 \pmod{p}$, which exists because p is an odd prime. This shows that $f \in (g_1, g_2)$ and that $g_2 \in \mathfrak{i}$. We only have to take care of $x^{p^{k_x}} - 1$ and g_3 now.

It is convenient to work with the variables $u = x - 1$ and $v = y - 1$, with lexicographic monomial order $u \succ v$. In terms of these variables, the ideal is $\mathfrak{i} = (\tilde{f}, u^{p^{k_x}}, v^{p^{k_y}})$, where $\tilde{f}(u, v) = f(u+1, v+1)$, and we have

$$\tilde{g}_1 = v^{3^{k_y}}, \quad \tilde{g}_2 = u^2 + u \left(-v + 4 \sum_{i=2}^{p^{k_y}-1} (-av)^i \right) + 4 \sum_{i=2}^{p^{k_y}-1} (-av)^i, \quad \tilde{g}_3 = uv^{p^{k_y}-1}. \quad (\text{B35})$$

where, once again, a is the reciprocal of 2 modulo p , and \tilde{g}_3 is needed only when $p > 3$ and $k_x = k_y$ as we will show below.

Let us show that $u^{p^{k_x}}$ is contained in the ideal generated by the Gröbner basis. Consider a polynomial of the form

$$s = \sum_{i=0}^k u^{k-i} v^i s_i(v), \quad (\text{B36})$$

where $s_i(v)$ are polynomials in v independent of u . For example, $u^{p^{k_x}}$ and $\tilde{g}_2 = u^2 + uvh_1(v) + v^2h_2(v)$ are both of this form,

¹⁹ Note that this Gröbner basis is minimal but not reduced, i.e., we can reduce the subleading terms of g_2 with respect to g_3 , but we choose not to do so. This does not affect any of our conclusions.

where $h_{1,2}(v)$ are polynomials in v . We want to reduce s with respect to \tilde{g}_2 as much as possible. First, we have

$$s^{(1)} = s - s_0(v)u^{k-2}\tilde{g}_2 = u^{k-1}v[s_1(v) - s_0(v)h_1(v)] + u^{k-2}v^2[s_2(v) - s_0(v)h_2(v)] + \sum_{i=3}^k u^{k-i}v^i s_i(v). \quad (\text{B37})$$

Clearly, $s^{(1)}$ is also of the same form as s but the leading term of $s^{(1)}$ is smaller than that of s . Repeating this $k-1$ times, we end up with the polynomial $s^{(k-1)}(u, v)$ of the form $uv^{k-1}s_{k-1}^{(k-1)}(v) + v^k s_k^{(k-1)}(v)$, which is not reducible with respect to \tilde{g}_2 anymore.

Applying this procedure to $u^{p^{k_x}}$, we get a polynomial of the form $uv^{p^{k_x}-1}r_1(v) + v^{p^{k_x}}r_2(v)$. When $k_x > k_y$, both terms are reducible with respect to \tilde{g}_1 , which means $u^{p^{k_x}}$ is in the ideal generated by \tilde{g}_1 and \tilde{g}_2 , and we are done. In particular, we do not need to add \tilde{g}_3 to the Gröbner basis.

On the other hand, when $k_x = k_y$, things are a bit more subtle. The second term is still reducible with respect to \tilde{g}_1 , but the first term is reducible with respect to \tilde{g}_1 if and only if $r_1(0) = 0$, i.e., the constant term of $r_1(v)$ vanishes (the non-constant terms are reducible with respect to \tilde{g}_1). If $r_1(0) \neq 0$, however, then we need \tilde{g}_3 to reduce the first term to 0. We will show that $r_1(0) = 0$ only when $p = 3$.

Let $\hat{g}_2 = u^2 + uvh_1(0) + v^2h_2(0) = u^2 - uv + v^2 = (u - av)^2 + bv^2 \pmod p$, where $b = 1 - a^2 = 3a^2 \pmod p$. Repeating the above reduction procedure on $u^{p^{k_y}}$ with respect to \hat{g}_2 , we again get a polynomial of the form $uv^{p^{k_y}-1}\hat{r}_1(v) + v^{p^{k_y}}\hat{r}_2(v)$. Moreover, it is clear that $\hat{r}_{1,2}(v)$ is obtained from $r_{1,2}(v)$ by replacing $h_{1,2}(v)$ with $h_{1,2}(0)$. This means, $r_{1,2}(0) = \hat{r}_{1,2}(0)$. Now, consider the equation

$$u^{p^{k_y}} = (u - av)^{p^{k_y}} + (av)^{p^{k_y}} = (u - av)(\hat{g}_2 - bv^2)^{(p^{k_y}-1)/2} + (av)^{p^{k_y}}. \quad (\text{B38})$$

This means, after reducing $u^{p^{k_y}}$ with respect to \hat{g}_2 , we get

$$(-b)^{(p^{k_y}-1)/2}(u - av)v^{p^{k_y}-1} - (av)^{p^{k_y}} \implies \hat{r}_1(v) = (-b)^{(p^{k_y}-1)/2}. \quad (\text{B39})$$

When $p = 3$, we have $b = 0 \implies \hat{r}_1(0) = 0 \implies r_1(0) = 0$, so $u^{3^{k_y}} \in (\tilde{g}_1, \tilde{g}_2)$, and there is no need to include \tilde{g}_3 in the Gröbner basis. On the other hand, when $p > 3$, we have $b = 3a^2 \not\equiv 0 \pmod p \implies \hat{r}_1(0) \neq 0 \implies r_1(0) \neq 0$, so

$$u^{p^{k_y}} = r_1(0)uv^{p^{k_y}-1} \pmod{(\tilde{g}_1, \tilde{g}_2)}. \quad (\text{B40})$$

This additional term is reducible with respect to \tilde{g}_3 , so $u^{p^{k_y}} \in (\tilde{g}_1, \tilde{g}_2, \tilde{g}_3)$.

Finally, we need to show that $\tilde{g}_3 \in \mathfrak{i}$ when $k_x = k_y$ and $p > 3$. Since $r_1(0) \neq 0 \pmod p$ in this case, the above equation can be rewritten as

$$\tilde{g}_3 = r_1(0)^{-1}u^{p^{k_y}} \pmod{(\tilde{f}, v^{p^{k_y}})}, \quad (\text{B41})$$

where we used the fact that $\tilde{g}_1, \tilde{g}_2 \in (\tilde{f}, v^{p^{k_y}})$. Therefore, $\tilde{g}_3 \in \mathfrak{i}$, and we are done. \square

Now we generalize the special case $L'_x = L'_y = 1$ to $L'_x = L'_y = q$, where $q > 2$ is a prime such that p is a primitive root modulo q^{20} . The equations (B25) become

$$f(x, y) = x^q - 1 = y^q - 1 = 0. \quad (\text{B42})$$

Let us prove that $x_0 = y_0 = 1$ is the only solution by contradiction. Assume that there exists another solution (x_0, y_0) with $x_0 \neq 1$. Since $x_0^q = 1$ and $x_0 \neq 1$, powers of x_0 generate all the q -th roots of 1. Hence $y_0 = x_0^s$ with $0 < s < q$, where s cannot take 0 since there is no solution of (B42) of the form $(x_0, 1)$ with $x_0 \neq 1$. Furthermore, (B42) is invariant under the transformation $y_0 \leftrightarrow y_0^{-1}$. So (x_0, x_0^{q-s}) is also a solution. We can then obtain a solution of the form (x_0, x_0^s) with $1 \leq s \leq (q-1)/2$. Now $f(x, y) = 0$ can be rewritten as $f(x, x^s) = 0$ where x_0 is a solution of it. Explicitly,

$$f(x, y) = x(y-1)^2 + y(x-1)^2 + (x-y)^2 \implies f(x, x^s) = x(x-1)^2 \tilde{f}_s(x), \quad (\text{B43})$$

²⁰ p is a primitive root modulo q if for every integer c coprime to q , there exists an integer n such that $p^n = c \pmod q$, or equivalently, p is the generator of the multiplicative group of integers modulo q , denoted as \mathbb{Z}_q^\times .

where

$$\tilde{f}_s(x) = \left(\sum_{i=0}^{s-1} x^i \right)^2 + x^{s-1} + x \left(\sum_{i=0}^{s-2} x^i \right)^2. \quad (\text{B44})$$

In $\mathbb{Z}_p[x]$, $\tilde{f}_s(x)$ is nonzero because $\tilde{f}_s(0) = 1 \pmod p$ for $s > 1$ and $2 \pmod p$ for $s = 1$. Clearly, x_0 must be a solution of $\tilde{f}_s(x)$ since $x_0 \neq 0, 1$. But x_0 is also a root of the cyclotomic polynomial $\Phi_q(x) = \sum_{i=0}^{q-1} x^i$. Now we use the fact that $\Phi_q(x)$ must be a minimal polynomial of x in $\mathbb{Z}_p[x]$ since p is a primitive root modulo q [56, Section 11.2.B]. This means $\tilde{f}_s(x)$ must be divisible by $\Phi_q(x)$. However,

$$\deg_x \tilde{f}_s(x) = 2s - 2 \leq q - 3 < q - 1 = \deg_x \Phi_q(x), \quad (\text{B45})$$

which is impossible, so there is no such x_0 . Therefore, $x_0 = y_0 = 1$ is the only solution in this case and $\log_p \text{GSD}_{\text{tri}}$ is again given by (B28) and (B33).

Finally, we further generalize the case to $L'_x = L'_y = q^m$, where $q > 2$ is a prime and m is a positive integer such that p is a primitive root modulo q^m . Then, the equations (B25) become

$$f(x, y) = x^{q^m} - 1 = y^{q^m} - 1 = 0. \quad (\text{B46})$$

Again, we assume there exists the solution other than $(1, 1)$ that can be written as (x_0, x_0^s) for $1 \leq s \leq (q^m - 1)/2$ by a similar argument as before. The range of s can be further narrowed down to $1 \leq s \leq (q^r - 1)/2$ where we assume there exists $0 < r \leq m$ such that $x_0^{q^r} = 1$ but $x_0^{q^{r'}} \neq 1$ for $r' < r$. We exclude the case $r = 0$ since it corresponds to the solution $(1, 1)$. According to the Euler totient function $\varphi(q^m) = q^m - q^{m-1}$, we separate the discussion into two cases:

- (1) $1 \leq s \leq \varphi(q^r)/2$: Since $x_0^{q^r} = 1$, x_0 is a root of the cyclotomic polynomial $\Phi_{q^r}(x) = \sum_{i=0}^{q^r-1} x^{iq^{r-1}}$. Meanwhile, since $x_0 \neq 0, 1$, it is also a root of $\tilde{f}_s(x)$ in (B43). Again, we use the fact that $\Phi_{q^r}(x)$ is a minimal polynomial of x_0 in $\mathbb{Z}_p[x]$ [?], so $\Phi_{q^r}(x)$ must divide $\tilde{f}_s(x)$. But this is impossible since

$$\deg_x \tilde{f}_s(x) = 2s - 2 \leq \varphi(q^r) - 2 < \varphi(q^r) = \deg_x \Phi_{q^r}(x). \quad (\text{B47})$$

Therefore, such an x_0 does not exist.

- (2) $\varphi(q^r)/2 < s \leq (q^r - 1)/2$: For convenience, let $t = q^r - 2s$ so that the range of t is $1 \leq t < q^{r-1} \leq (q^r - q^{r-1})/2 = \varphi(q^r)/2$ where the rightmost inequality holds for $q > 2$. There is a $z_0 \in \mathbb{F}$ such that $z_0^{q^r} = 1$ but $z_0^{q^{r'}} \neq 1$ for $r' < r$, and $x_0 = z_0^2$ (which is possible because $q > 2$). Then, the solution (x_0, x_0^s) is of the form (z_0^2, z_0^{2s}) . The transformation $y_0 \leftrightarrow y_0^{-1}$ implies (z_0^2, z_0^t) is also a solution. It follows that z_0 is a root of

$$f(x^2, x^t) = \begin{cases} x(x-1)^2 \tilde{f}_1(x), & t = 1, \\ x^2(x-1)^2 \tilde{f}_t(x), & t > 1, \end{cases} \quad (\text{B48})$$

where

$$\tilde{f}_t(x) = \begin{cases} x + (x+1)^2 + x, & t = 1 \\ \left(\sum_{i=0}^{t-1} x^i \right)^2 + x^{t-2}(x+1)^2 + x^2 \left(\sum_{i=0}^{t-3} x^i \right)^2, & t > 1, \end{cases} \quad (\text{B49})$$

Note that $\tilde{f}_t(x)$ is nonzero because $\tilde{f}_t(0) = 1 \pmod p$ for $t \neq 2$ and $2 \pmod p$ for $t = 2$. Meanwhile, as z_0 is a root of $f(x^2, x^t)$ and $z_0 \neq 0, 1$, it is also a root of $\tilde{f}_t(x)$. Again, we use the fact that $\Phi_{q^r}(x)$ is a minimal polynomial of z_0 , so $\Phi_{q^r}(x)$ must divide $\tilde{f}_t(x)$. But this is impossible because

$$\deg_x \tilde{f}_t(x) = 2t - 2 + 2\delta_{t,1} \leq 2t < \varphi(q^r) = \deg_x \Phi_{q^r}(x). \quad (\text{B50})$$

Thus, there is no such z_0 .

Therefore, when p is a primitive root modulo q^m , $(1, 1)$ is the only solution of (B46). Hence, $\log_p \text{GSD}_{\text{tri}}$ is still given by (B28) and (B33).

To conclude, when $L_x = p^{k_x} q^m$ and $L_y = p^{k_y} q^m$, where $k_x, k_y, m \geq 0$ are integers and q is an odd prime such that p is a

primitive root modulo q^m (for $m \geq 1$), the ground-state of the triangular-based \mathbb{Z}_p Laplacian model is given by

$$\log_p \text{GSD}_{\text{tri}} = \begin{cases} 2 \times 3^{\min(k_x, k_y)}, & p = 3, \\ 2p^{\min(k_x, k_y)} - \delta_{k_x, k_y}, & p > 3. \end{cases} \quad (\text{B51})$$

3. \mathbb{Z}_3 fractal spin liquid

Once again, $q = t = 1$ in this case, so we use (B13) to compute the GSD for some special values of L_x and L_y . The ideal is $\mathfrak{i} = (f, x^{L_x} - 1, y^{L_y} - 1)$, where $f(x, y) = 1 + x + y$. Like before, we consider the factorization $x^{L_x} - 1 = (x^{L'_x} - 1)^{3^{k_x}}$, $y^{L_y} - 1 = (y^{L'_y} - 1)^{3^{k_y}}$ and take the special case $L'_x = L'_y = 1$. The system of polynomial equations we need to solve is

$$1 + x + y = x - 1 = y - 1 = 0. \quad (\text{B52})$$

Clearly, the only solution is $(1, 1)$, so the ideal is $(1 + x + y, x^{3^{k_x}} - 1, y^{3^{k_y}} - 1)$. Assuming without loss of generality that $k_x \geq k_y$, the Gröbner basis is easily seen to be

$$g_1 = y^{3^{k_y}} - 1, \quad g_2 = x + y + 1. \quad (\text{B53})$$

The only slightly nontrivial fact to verify is that

$$x^{3^{k_x}} - 1 = (g_2 - y - 1)^{3^{k_x}} - 1 = g_2^{3^{k_x}} - (y^{3^{k_x}} - 1) = 0 \pmod{(g_1, g_2)}. \quad (\text{B54})$$

The set of monomials which are irreducible with respect to the Gröbner basis is

$$\{1, y, \dots, y^{3^{k_y}-1}\}, \quad (\text{B55})$$

with cardinality 3^{k_y} . By (B13),

$$\log_3 \text{GSD}_{\text{FSL}} = 3^{k_y}. \quad (\text{B56})$$

We use the same argument as before to generalize the simplest case $L'_x = L'_y = 1$ to the more general case $L'_x = L'_y = q$ where q is an odd prime such that 3 is a primitive root modulo q (e.g., $q = 5$). Assume there exists a solution other than $(1, 1)$ which can be written as (x_0, x_0^s) with $x_0 \neq 1$ and $1 \leq s \leq (q-1)/2$ by the same reasoning as in Appendix B 2. Then x_0 is a root of

$$f(x, x^s) = 1 + x + x^s = (x-1)\tilde{f}_s(x), \quad \tilde{f}_s(x) = 1 + \sum_{i=0}^{s-1} x^i. \quad (\text{B57})$$

Clearly, $\tilde{f}_s(x)$ is nonzero since $\tilde{f}_s(0) = -1 \pmod{3}$. And since $x_0 \neq 1$, x_0 must be a solution of $\tilde{f}_s(x)$. Again, the cyclotomic polynomial $\Phi_q(x)$ is a minimal polynomial of x_0 in $\mathbb{Z}_3[x]$, so it must divide $\tilde{f}_s(x)$. But this is impossible since

$$\deg \tilde{f}_s(x) = s - 1 \leq \frac{q-3}{2} < q-1 = \deg_x \Phi_q(x). \quad (\text{B58})$$

So there is no such x_0 , and hence $\log_3 \text{GSD}_{\text{FSL}}$ is given by (B56).

Generalizing further, let $L'_x = L'_y = q^m$, where m is a positive integer and q is an odd prime such that 3 is a primitive root modulo q^m (e.g., $q = 5$ and any $m \geq 1$). Assume there exists a solution of the form $(x_0, x_0^s) \neq (1, 1)$ for $1 \leq s \leq (q^r - 1)/2$ where $0 < r \leq m$ and $x_0^{q^r} = 1$ but $x_0^{q^{r'}} \neq 1$ for $r' < r$.

(1) $1 \leq s \leq \varphi(q^r)/2$: x_0 is a root of the cyclotomic polynomial $\Phi_{q^r}(x)$ and $\tilde{f}_s(x)$ in (B57). But $\Phi_{q^r}(x)$ is a minimal polynomial of x_0 in $\mathbb{Z}_3[x]$ so it must divide $\tilde{f}_s(x)$, which is impossible since

$$\deg \tilde{f}_s(x) = \varphi(q^r)/2 - 1 < \varphi(q^r) = \deg_x \Phi_{q^r}(x). \quad (\text{B59})$$

So there is no such x_0 .

(2) $\varphi(q^r)/2 < s < (q^r - 1)/2$: Again, we let $t = q^r - 2s$ so that we have $1 \leq t < \varphi(q^r)/2$. By the same reasoning as before,

we can write $x_0 = z_0^2$ and so (z_0^2, z_0^t) is a solution. Thus z_0 is a root of

$$f(x^2, x^t) = 1 + x^2 + x^t = (x-1)\tilde{f}_t(x), \quad \tilde{f}_t(x) = x + 1 + \sum_{i=0}^{t-1} x^i. \quad (\text{B60})$$

Note that $\tilde{f}_t(x)$ is nonzero as $\tilde{f}_t(0) = -1 \pmod{3}$. Because z_0 is a root of $f(x^2, x^t)$ and $z_0 \neq 1$, it is also a root of $\tilde{f}_t(x)$. Again, $\Phi_{q^r}(x)$ is a minimal polynomial of z_0 in $\mathbb{Z}_3[x]$ so that it must divide $\tilde{f}_s(x)$. But this is impossible since

$$\deg_x \tilde{f}_t(x) = t - 1 + \delta_{t,1} \leq t < \varphi(q^r) = \deg_x \Phi_{q^r}(x). \quad (\text{B61})$$

So there is no such z_0 .

Therefore, when 3 is a primitive root modulo q^m , $(1, 1)$ is the solution of (B52). Hence, $\log_3 \text{GSD}_{\text{FSL}}$ is still given by (B56).

To conclude, when $L_x = 3^{k_x} q^m$ and $L_y = 3^{k_y} q^m$ where $k_x, k_y, m \geq 0$ are integers and q is an odd prime such that p is a primitive root modulo q^m (e.g., $q = 5$ and any $m \geq 1$), the ground-state degeneracy of the \mathbb{Z}_3 fractal spin liquid is given by

$$\log_3 \text{GSD}_{\text{FSL}} = 3^{\min(k_x, k_y)}. \quad (\text{B62})$$

4. \mathcal{B} code of \mathbb{Z}_3 Laplacian model on the square lattice

In this case, $q = t = 2$, and the stabilizer matrix is given by (54)

$$\mathcal{B}_{\text{sq}}^{\mathbb{Z}_3} = \begin{pmatrix} (\mathcal{B}_{\text{sq}}^{\mathbb{Z}_3})^Z \\ 0 \end{pmatrix}, \quad (\mathcal{B}_{\text{sq}}^{\mathbb{Z}_3})^Z = \begin{pmatrix} -x + y & 1 - x \\ -y + xy & 1 - xy \end{pmatrix}. \quad (\text{B63})$$

So we use (B22) to compute the GSD for some special values of L_x and L_y . The ideal is $\mathfrak{i} = (f, x^{L_x} - 1, y^{L_y} - 1)$, where $f(x, y) = -\det(\mathcal{B}_{\text{sq}}^{\mathbb{Z}_3})^Z = x(y-1)^2 + y(x-1)^2 \pmod{3}$ is precisely the polynomial in (A1)²¹. Once again, consider the factorization $x^{L_x} - 1 = (x^{L'_x} - 1)^{3^{k_x}}$, $y^{L_y} - 1 = (y^{L'_y} - 1)^{3^{k_y}}$ and take $L'_x = L'_y = q^m$, where $k_x, k_y, m \geq 0$ are integers and q is an odd prime such that 3 is a primitive root modulo q^m for $m \geq 1$ (e.g., $q = 5$ and any $m \geq 1$). Then, the system of polynomial equations we need to solve is

$$f(x, y) = x^{q^m} - 1 = y^{q^m} - 1 = 0. \quad (\text{B64})$$

In [1], it was shown that this system has only the trivial solution $(1, 1)$. Therefore, the GSD is given by

$$\log_3 \text{GSD}_{\mathcal{B}, \text{sq}} = \dim_{\mathbb{F}} \mathbb{F}[x, y]^2 / \text{im } \tau, \quad (\text{B65})$$

where²²

$$\tau = \begin{pmatrix} x - y & 1 - x & x^{3^{k_x}} - 1 & 0 & y^{3^{k_y}} - 1 & 0 \\ xy - y & xy - 1 & 0 & x^{3^{k_x}} - 1 & 0 & y^{3^{k_y}} - 1 \end{pmatrix}. \quad (\text{B66})$$

Assuming without loss of generality that $k_x \geq k_y$, the Gröbner basis of $\text{im } \tau$ is given by

$$\mathbf{g}_1 = \begin{pmatrix} y^{3^{k_y}} - 1 \\ 0 \end{pmatrix}, \quad \mathbf{g}_2 = \begin{pmatrix} 0 \\ y^{3^{k_y}} - 1 \end{pmatrix}, \quad \mathbf{g}_3 = \begin{pmatrix} x + y + 1 \\ y - 1 \end{pmatrix}, \quad \mathbf{g}_4 = \begin{pmatrix} -y^{3^{k_y}-1} + 1 \\ x + y^{3^{k_y}-1} + 1 \end{pmatrix}. \quad (\text{B67})$$

²¹ More precisely, the ideal is $(\bar{f}, x^{L_x} - 1, y^{L_y} - 1)$ because $\det((\mathcal{B}_{\text{sq}}^{\mathbb{Z}_3})^Z)^\dagger = -\bar{f}(x, y) = -\bar{f}(\bar{x}, \bar{y}) = -\bar{x}^2 \bar{y}^2 f(x, y)$, which is the equivalent to $-f(x, y)$ up to a monomial (i.e., translations).

²² The first two columns of this matrix are given by $xy \times ((\mathcal{B}_{\text{sq}}^{\mathbb{Z}_3})^Z)^\dagger$.

The set of monomials of $\mathbb{F}[x, y]^2$ that are irreducible with respect to this Gröbner basis is

$$\left\{ \begin{pmatrix} 1 \\ 0 \end{pmatrix}, \dots, \begin{pmatrix} y^{3^{k_y}-1} \\ 0 \end{pmatrix}, \begin{pmatrix} 0 \\ 1 \end{pmatrix}, \dots, \begin{pmatrix} 0 \\ y^{3^{k_y}-1} \end{pmatrix} \right\}, \quad (\text{B68})$$

with cardinality 2×3^{k_y} . By (B22), the GSD is

$$\log_3 \text{GSD}_{\mathcal{B}, \text{sq}} = 2 \times 3^{\min(k_x, k_y)}. \quad (\text{B69})$$

Proof of Gröbner basis. It is easy to check that the above Gröbner basis satisfies the Buchberger's criterion. It is also easy to see that

$$\begin{aligned} \mathbf{g}_3 &= \tau_2 - \tau_1, & \mathbf{g}_4 &= -y^{3^{k_y}-1}(\tau_1 + \tau_2) - \tau_5 - (x+1)\tau_6, \\ \tau_1 &= \mathbf{g}_1 - \mathbf{g}_2 + \mathbf{g}_3 + y\mathbf{g}_4, & \tau_2 &= \mathbf{g}_1 - \mathbf{g}_2 - \mathbf{g}_3 + y\mathbf{g}_4. \end{aligned} \quad (\text{B70})$$

where τ_i denotes the i -th column of τ . Therefore, $\{\mathbf{g}_1, \dots, \mathbf{g}_4\} \in \text{im } \tau$ and $\tau_1, \tau_2 \in \langle \mathbf{g}_1, \dots, \mathbf{g}_4 \rangle$. All that is left is to show that $\tau_3, \tau_4 \in \langle \mathbf{g}_1, \dots, \mathbf{g}_4 \rangle$.

It is convenient to work with variables $u = x - 1$ and $v = y - 1$ with monomial order $u \succ v$. Then the matrix τ becomes

$$\tilde{\tau} = \begin{pmatrix} u-v & -u & u^{3^{k_x}} & 0 & v^{3^{k_y}} & 0 \\ uv+u & uv+u+v & 0 & u^{3^{k_x}} & 0 & v^{3^{k_y}} \end{pmatrix}, \quad (\text{B71})$$

and the Gröbner basis is

$$\tilde{\mathbf{g}}_1 = \begin{pmatrix} v^{3^{k_y}} \\ 0 \end{pmatrix}, \quad \tilde{\mathbf{g}}_2 = \begin{pmatrix} 0 \\ v^{3^{k_y}} \end{pmatrix}, \quad \tilde{\mathbf{g}}_3 = \begin{pmatrix} u+v \\ v \end{pmatrix}, \quad \tilde{\mathbf{g}}_4 = \begin{pmatrix} v \sum_{i=0}^{3^{k_y}-2} (-v)^i \\ u - v \sum_{i=0}^{3^{k_y}-2} (-v)^i \end{pmatrix}. \quad (\text{B72})$$

Consider a general vector of the form

$$\mathbf{s} = \sum_{i=0}^k u^{k-i} v^i \begin{pmatrix} s_{1,i}(v) \\ s_{2,i}(v) \end{pmatrix}, \quad (\text{B73})$$

where $s_{1,i}(v)$ and $s_{2,i}(v)$ are polynomials in v independent of u . For example, $\tilde{\tau}_3$, $\tilde{\tau}_4$, $\tilde{\mathbf{g}}_3$, and $\tilde{\mathbf{g}}_4$ are all of this form. We want to reduce \mathbf{s} with respect to $\tilde{\mathbf{g}}_3$ and $\tilde{\mathbf{g}}_4$ as much as possible. First, we have

$$\mathbf{s}^{(1)} = \mathbf{s} - s_{1,0}(v)u^{k-1}\tilde{\mathbf{g}}_3 - s_{2,0}(v)u^{k-1}\tilde{\mathbf{g}}_4. \quad (\text{B74})$$

It is easy to see that $\mathbf{s}^{(1)}$ is of the same form as \mathbf{s} and the leading terms of both components of $\mathbf{s}^{(1)}$ are smaller than the leading terms of the corresponding components of \mathbf{s} . Repeating this k times, we end up with a vector of the form

$$\mathbf{s}^{(k)} = v^k \begin{pmatrix} s_{1,k}^{(k)}(v) \\ s_{2,k}^{(k)}(v) \end{pmatrix}, \quad (\text{B75})$$

which is not reducible with respect to $\tilde{\mathbf{g}}_3$ or $\tilde{\mathbf{g}}_4$ anymore.

Applying this procedure to $\tilde{\tau}_3$ and $\tilde{\tau}_4$, we end up with a vector proportional to $v^{3^{k_x}}$, which is reducible with respect to $\tilde{\mathbf{g}}_1$ and $\tilde{\mathbf{g}}_2$ because $k_x \geq k_y$. Therefore, $\tilde{\tau}_3, \tilde{\tau}_4 \in \langle \tilde{\mathbf{g}}_1, \dots, \tilde{\mathbf{g}}_4 \rangle$. \square

Appendix C: Mobility of z -lineons in the triangular-based anisotropic Laplacian model

As mentioned in the main text, the point-like excitations of the anisotropic Laplacian model can always move in the z direction, making them z -lineons. Their mobility in the xy

plan is quite nontrivial and can be analyzed in the polynomial formalism [4]. Consider a configuration of Q z -lineons with positions (n_i, m_i) , described by the Laurent polynomial (i.e.,

an element of $\mathbb{Z}_N[x, x^{-1}, y, y^{-1}]$,

$$q(x, y) = \sum_{i=1}^Q x^{n_i} y^{m_i}. \quad (\text{C1})$$

Assume this configuration of Q lineons can rigidly move to another position $(n_0, m_0) \neq (0, 0)$. This is equivalent to the existence of a Laurent polynomial $s(x, y)$ such that [1, 40]

$$(x^{n_0} y^{m_0} - 1)q(x, y) = s(x, y)f(x, y) \pmod{N}. \quad (\text{C2})$$

Here, $f(x, y) = x^2 + y^2 + x^2 y + x y^2 + x + y - 6xy$ is the stabilizer polynomial given by the top left entry of (29). Physically, (C2) means that the configurations at the initial position $(0, 0)$ and the final position (n_0, m_0) can be connected by the Hamiltonian terms (trivial charge configurations) $f(x, y)$ without creating additional excitations.

If $q(x, y)$ can be written as $q(x, y) = r(x, y)f(x, y)$ for some Laurent polynomial $r(x, y) = \sum_j x^{n'_j} y^{m'_j}$, then the condition (C2) is trivially satisfied by choosing $s(x, y) = (x^{n_0} y^{m_0} - 1)r(x, y)$. A more interesting case is when $q(x, y) \neq r(x, y)f(x, y)$ for any $r(x, y)$, which means $f(x, y)$ and $x^{n_0} y^{m_0} - 1$ must share a nontrivial factor.

When $N = 2$, the stabilizer polynomial can be factorized into $f(x, y) = (x + y)(1 + x)(1 + y) \pmod{2}$. Taking $(n_0, m_0) = (n, -n)$, $x^n y^{-n} + 1$ can be factorized as

$$(x + y)(x^{n-1} + x^{n-2}y + \dots + y^{n-1}) \pmod{2}, \quad (\text{C3})$$

up to a monomial y^{-n} . The condition (C2) is thus satisfied when $q(x, y) = (1 + x)(1 + y) = 1 + x + y + xy$. That is, a quadrupole of z -lineons located at the relative positions $(0, 0)$, $(1, 0)$, $(0, 1)$ and $(1, 1)$ can move along the $(\pm 1, \mp 1)$ direction, as illustrated in Fig. 3. Using the above factorization of $f(x, y)$, we can further show that there are two other mobile configurations: a quadrupole of $(0, 0)$, $(1, 0)$, $(0, 1)$, $(-1, 1)$, and that of $(0, 0)$, $(0, 1)$, $(-1, 1)$, $(-1, 2)$ can move in the $(0, \pm 1)$ and $(\pm 1, 0)$ directions, respectively.

When $N = p$ is an odd prime, we show that the condition (C2) cannot be satisfied, except trivially as in $q(x, y) = r(x, y)f(x, y)$. Let p^k be the largest power of p that divides n_0 and m_0 , i.e., $n'_0 = n_0/p^k$, $m'_0 = m_0/p^k$, and $d = \gcd(n'_0, m'_0)$ is not divisible by p . First we observe that $x^{n_0} y^{m_0} - 1$ can be factorized as

$$(x^{n'_0} y^{m'_0} - 1)^{p^k} = [(x^{n'_0} y^{m'_0} - 1)t(x, y)]^{p^k} \pmod{p}, \quad (\text{C4})$$

where $n''_0 = n'_0/d$, $m''_0 = m'_0/d$ and $t(x, y) = \sum_{i=0}^{d-1} (x^{n''_0} y^{m''_0})^i$. Specifically, for $N = 3$, the stabilizer polynomial $f(x, y)$ is factorizable as $(1 + x + y)(x + y + xy) \pmod{3}$. All we need to show is that $x^{n_0} y^{m_0} - 1$ is not a multiple of $f_1(x, y) = 1 + x + y$ or $f_2(x, y) = x + y + xy$. Note that $t(1, 1) = d \neq 0 \pmod{3}$ but $f_1(1, 1) = f_2(1, 1) = 0 \pmod{3}$. Therefore, $t(x, y)^{p^k}$ is not a multiple of $f_1(x, y)$ and $f_2(x, y)$. Also $x^{n'_0} y^{m'_0} - 1$ is irreducible up to a monomial so $(x^{n'_0} y^{m'_0} - 1)^{p^k}$ is also not a multiple of either of them. Therefore, $x^{n_0} y^{m_0} - 1$ is not a multiple of $f(x, y)$ for $N = 3$.

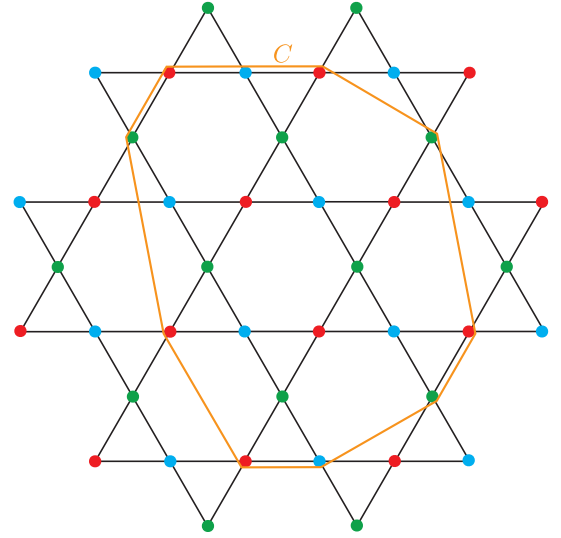


FIG. 10. A simple closed convex polygonal curve C whose corners are on the sites of the Kagome lattice. We enlarged the curve a bit so that the sites and links along the boundary are visible.

When $N = p > 3$, the stabilizer polynomial $f(x, y)$ is irreducible up to a monomial.²³ Using the same argument again, we can show that $x^{n_0} y^{m_0} - 1$ is not a multiple of $f(x, y)$.

In conclusion, we find that any finite set of z -lineons in the triangular-based anisotropic \mathbb{Z}_p Laplacian model with odd prime p cannot move in the xy plane, except when they are created locally.

Appendix D: Robustness of the anisotropic Laplacian model on various regular lattices

In this appendix, we prove the robustness of the anisotropic \mathbb{Z}_N Laplacian model on the extended triangular, honeycomb, and Kagome lattices. We will show that, on the Kagome lattice, robustness requires N to be coprime to 6, but there are no such restrictions on N on the triangular and honeycomb lattices.

As explained in Sec. III A, the logical operators W_z and \tilde{W}_z have non-local support, so let us focus on $W(h)$ and $\tilde{W}(h)$, whose support is the same as that of the discrete harmonic function h .

Assume h has finite support. Consider a simple closed convex polygonal curve C whose corners are on the lattice sites and whose interior contains the support of h (points on C are considered to be inside C). An example curve on Kagome lattice is sketched in Fig. 10. It is easy to see that every corner of C has at least two neighbouring sites outside C (a.k.a. outer neighbours). Pick a corner i of C . We have two cases.

²³ For $p > 5$, the irreducibility of $f(x, y)$ modulo p can be verified using [57, Corollary 3]. For $p = 5$, this can be done in a computer algebra system, such as Mathematica.

1. There is an outer neighbour of i , call it j , such that the remaining three neighbours of j are all outside C . (This is always the case on the triangular and honeycomb lattices, but not on the Kagome lattice—e.g., this is the case for all the corners of C in Fig. 10 except for the red and green corners on the top-left.) In this case, using the discrete Laplacian equation $\Delta_L h(j) = 0 \pmod N$ at the site j , we find that $h(i) = 0 \pmod N$. So we can shrink C inward to get a curve with smaller interior but still contains the support of h .
2. On the Kagome lattice, if the condition of the last case is not satisfied, then there are two outer neighbours of i , call them j_1 and j_2 , such that j_1 (resp. j_2) has another neighbour i_1 (resp. i_2) inside C . (This is the case, for example, for the red and green corners on the top-left of C in Fig. 10.) In this case, using the discrete Laplacian

equation at the sites j_1 and j_2 , we get $h(i) = -h(i_1) = -h(i_2) \pmod N$. Combining these equations with the discrete Laplacian equation at the site i , we find that $6h(i) = 0 \pmod N$. When N is coprime to 6, we get $h(i) = 0 \pmod N$, which also implies that $h(i_1) = h(i_2) = 0 \pmod N$. Therefore, once again, we can shrink C inward to get a curve with smaller interior but still contains the support of h .

Repeating these steps, by induction, we conclude that $h = 0$ everywhere. Hence, the anisotropic \mathbb{Z}_N Laplacian model on triangular and honeycomb lattices is robust for all N , whereas it is robust on the Kagome lattice if and only if N is coprime to 6. (Recall that, in Sec. III C, we constructed local logical operators on the Kagome lattice when N is a multiple of 2 or 3.)

-
- [1] P. Gorantla, H. T. Lam, N. Seiberg, and S.-H. Shao, Gapped lineon and fracton models on graphs, *Phys. Rev. B* **107**, 125121 (2023).
 - [2] C. Chamon, Quantum glassiness in strongly correlated clean systems: An example of topological overprotection, *Phys. Rev. Lett.* **94**, 040402 (2005).
 - [3] S. Vijay, J. Haah, and L. Fu, A new kind of topological quantum order: A dimensional hierarchy of quasiparticles built from stationary excitations, *Phys. Rev. B* **92**, 235136 (2015).
 - [4] S. Vijay, J. Haah, and L. Fu, Fracton topological order, generalized lattice gauge theory, and duality, *Phys. Rev. B* **94**, 235157 (2016).
 - [5] J. Haah, Local stabilizer codes in three dimensions without string logical operators, *Phys. Rev. A* **83**, 042330 (2011).
 - [6] A. Gromov and L. Radzihovsky, Colloquium: Fracton matter, *Rev. Mod. Phys.* **96**, 011001 (2024).
 - [7] R. M. Nandkishore and M. Hermele, Fractons, *Annual Review of Condensed Matter Physics* **10**, 295 (2019).
 - [8] M. Pretko, X. Chen, and Y. You, Fracton phases of matter, *International Journal of Modern Physics A* **35**, 2030003 (2020).
 - [9] H. Casasola, G. Delfino, P. R. S. Gomes, and P. F. Biezobaz, Fractal subsystem symmetries, 't hooft anomalies, and uv/ir mixing, *Phys. Rev. B* **109**, 075164 (2024).
 - [10] N. E. Myerson-Jain, S. Liu, W. Ji, C. Xu, and S. Vijay, Pascal's triangle fractal symmetries, *Phys. Rev. Lett.* **128**, 115301 (2022).
 - [11] G. Vidal, Entanglement renormalization, *Phys. Rev. Lett.* **99**, 220405 (2007).
 - [12] M. Aguado and G. Vidal, Entanglement renormalization and topological order, *Phys. Rev. Lett.* **100**, 070404 (2008).
 - [13] K. G. Wilson, The renormalization group: Critical phenomena and the kondo problem, *Rev. Mod. Phys.* **47**, 773 (1975).
 - [14] R. König, B. W. Reichardt, and G. Vidal, Exact entanglement renormalization for string-net models, *Phys. Rev. B* **79**, 195123 (2009).
 - [15] C. M. Dawson, J. Eisert, and T. J. Osborne, Unifying variational methods for simulating quantum many-body systems, *Phys. Rev. Lett.* **100**, 130501 (2008).
 - [16] M. Rizzi, S. Montangero, and G. Vidal, Simulation of time evolution with multiscale entanglement renormalization ansatz, *Phys. Rev. A* **77**, 052328 (2008).
 - [17] G. Evenbly and G. Vidal, Algorithms for entanglement renormalization, *Phys. Rev. B* **79**, 144108 (2009).
 - [18] R. N. C. Pfeifer, G. Evenbly, and G. Vidal, Entanglement renormalization, scale invariance, and quantum criticality, *Phys. Rev. A* **79**, 040301 (2009).
 - [19] J. Haegeman, T. J. Osborne, H. Verschelde, and F. Verstraete, Entanglement renormalization for quantum fields in real space, *Phys. Rev. Lett.* **110**, 100402 (2013).
 - [20] J. Haah, Bifurcation in entanglement renormalization group flow of a gapped spin model, *Phys. Rev. B* **89**, 075119 (2014).
 - [21] B. Zeng and X.-G. Wen, Gapped quantum liquids and topological order, stochastic local transformations and emergence of unitarity, *Phys. Rev. B* **91**, 125121 (2015).
 - [22] A. Kitaev, Fault-tolerant quantum computation by anyons, *Annals of Physics* **303**, 2 (2003).
 - [23] J. Haah, Classification of translation invariant topological Pauli stabilizer codes for prime dimensional qudits on two-dimensional lattices, *Journal of Mathematical Physics* **62**, 012201 (2021).
 - [24] H. Bombin, G. Duclos-Cianci, and D. Poulin, Universal topological phase of two-dimensional stabilizer codes, *New Journal of Physics* **14**, 073048 (2012).
 - [25] H. Bombin, Structure of 2d topological stabilizer codes, *Communications in Mathematical Physics* **327**, 387 (2014).
 - [26] W. Shirley, K. Slagle, and X. Chen, Fractional excitations in foliated fracton phases, *Annals of Physics* **410**, 167922 (2019).
 - [27] B. Yoshida, Exotic topological order in fractal spin liquids, *Phys. Rev. B* **88**, 125122 (2013).
 - [28] W. Shirley, K. Slagle, Z. Wang, and X. Chen, Fracton models on general three-dimensional manifolds, *Phys. Rev. X* **8**, 031051 (2018).
 - [29] W. Shirley, K. Slagle, and X. Chen, Foliated fracton order in the checkerboard model, *Phys. Rev. B* **99**, 115123 (2019).
 - [30] W. Shirley, K. Slagle, and X. Chen, Foliated fracton order from gauging subsystem symmetries, *SciPost Phys.* **6**, 041 (2019).
 - [31] W. Shirley, K. Slagle, and X. Chen, Universal entanglement signatures of foliated fracton phases, *SciPost Phys.* **6**, 015 (2019).
 - [32] A. Dua, P. Sarkar, D. J. Williamson, and M. Cheng, Bifurcating entanglement-renormalization group flows of fracton stabilizer models, *Phys. Rev. Res.* **2**, 033021 (2020).
 - [33] Z. Wang, X. Ma, D. T. Stephen, M. Hermele, and X. Chen,

- Renormalization of ising cage-net model and generalized foliation, *Phys. Rev. B* **108**, 035148 (2023).
- [34] G. Evenbly and G. Vidal, Real-space decoupling transformation for quantum many-body systems, *Phys. Rev. Lett.* **112**, 220502 (2014).
 - [35] G. Evenbly and G. Vidal, Class of highly entangled many-body states that can be efficiently simulated, *Phys. Rev. Lett.* **112**, 240502 (2014).
 - [36] G. Evenbly and G. Vidal, Scaling of entanglement entropy in the (branching) multiscale entanglement renormalization ansatz, *Phys. Rev. B* **89**, 235113 (2014).
 - [37] P. Gorantla, H. T. Lam, N. Seiberg, and S.-H. Shao, Low-energy limit of some exotic lattice theories and uv/ir mixing, *Phys. Rev. B* **104**, 235116 (2021).
 - [38] P. Gorantla, H. T. Lam, and S.-H. Shao, Fractons on graphs and complexity, *Phys. Rev. B* **106**, 195139 (2022).
 - [39] H. Ebisu and B. Han, Anisotropic higher rank \mathbb{Z}_N topological phases on graphs, *SciPost Phys.* **14**, 106 (2023).
 - [40] P. Gorantla, H. T. Lam, N. Seiberg, and S.-H. Shao, (2+1)-dimensional compact lifshitz theory, tensor gauge theory, and fractons, *Phys. Rev. B* **108**, 075106 (2023).
 - [41] N. Manoj and V. B. Shenoy, Arboreal topological and fracton phases, (2021), [arXiv:2109.04259](https://arxiv.org/abs/2109.04259).
 - [42] J. Haah, Commuting pauli hamiltonians as maps between free modules, *Communications in Mathematical Physics* **324**, 351 (2013).
 - [43] A. Steane, Multiple-particle interference and quantum error correction, *Proceedings of the Royal Society of London. Series A: Mathematical, Physical and Engineering Sciences* **452**, 2551 (1996).
 - [44] A. R. Calderbank and P. W. Shor, Good quantum error-correcting codes exist, *Phys. Rev. A* **54**, 1098 (1996).
 - [45] J. Haah, A degeneracy bound for homogeneous topological order, *SciPost Phys.* **10**, 011 (2021).
 - [46] C. Castelnovo and C. Chamon, Topological quantum glassiness, *Philosophical Magazine* **92**, 304 (2012).
 - [47] L. P. Kadanoff, Scaling laws for ising models near T_c , *Physics Physique Fizika* **2**, 263 (1966).
 - [48] T. Rudelius, N. Seiberg, and S.-H. Shao, Fractons with twisted boundary conditions and their symmetries, *Phys. Rev. B* **103**, 195113 (2021).
 - [49] N. Seiberg and S.-H. Shao, Exotic symmetries, duality, and fractons in 2+1-dimensional quantum field theory, *SciPost Phys.* **10**, 027 (2021).
 - [50] P. Gorantla, H. T. Lam, N. Seiberg, and S.-H. Shao, fcc lattice, checkerboards, fractons, and quantum field theory, *Phys. Rev. B* **103**, 205116 (2021).
 - [51] N. Tantivasadakarn, Jordan-wigner dualities for translation-invariant hamiltonians in any dimension: Emergent fermions in fracton topological order, *Phys. Rev. Res.* **2**, 023353 (2020).
 - [52] W. Shirley, Fractonic order and emergent fermionic gauge theory, (2020), [arXiv:2002.12026](https://arxiv.org/abs/2002.12026) [[cond-mat.str-el](https://arxiv.org/archive/cond)].
 - [53] H. Song, N. Tantivasadakarn, W. Shirley, and M. Hermele, Fracton self-statistics, *Phys. Rev. Lett.* **132**, 016604 (2024).
 - [54] Z.-C. Gu and X.-G. Wen, Tensor-entanglement-filtering renormalization approach and symmetry-protected topological order, *Phys. Rev. B* **80**, 155131 (2009).
 - [55] O. Lezama, Gröbner bases for the modules over noetherian polynomial commutative rings, *Georgian Mathematical Journal* **15**, 121 (2008).
 - [56] D. A. Cox, *Galois Theory*, 2nd ed. (John Wiley & Sons, New York, 2012).
 - [57] S. Gao and V. M. Rodrigues, Irreducibility of polynomials modulo p via newton polytopes, *Journal of Number Theory* **101**, 32 (2003).